Proteo-transcriptomic profiling of nasal mononuclear phagocytic system cells in human controlled allergen challenge.

Voskamp AL[1], Gerdes ML[2*], Menafra R[3*], Duijster E[4], Kielbasa SM[5], Groot Kormelink T[6], Tak T[1], Stam K[1], de Jong, NW[4], Hendricks RW[7], Kloet SL[3], Yazdanbakhsh M[1], de Jong EC[6], Gerth van Wijk R[4], Smits HH[1].

[1]Department of Parasitology, Leiden University Medical Center, Leiden, The Netherlands; [2]Dept of Ear, Nose and Throat, Erasmus Medical Center, Rotterdam, The Netherlands; [3]Leiden Genome Technology Center Leiden University Medical Center, Leiden, The Netherlands; [4]Dept of Internal Medicine, Section Allergology, Erasmus Medical Center, Rotterdam, The Netherlands; [5]Sequencing Analysis Support Core, Leiden University Medical Center, Leiden, The Netherlands, [6]Dept of Exp Immunology, Amsterdam University Medical Centers, Amsterdam, The Netherlands and [7]Dept. of Pulmonology, Erasmus Medical Center, Rotterdam, The Netherlands

Corresponding author:
Dr. H.H. Smits
Dept of Parasitology
LUMC Center of Infectious Diseases
Leiden University Medical Center (LUMC)
Albinusdreef 2
2333 ZA Leiden
The Netherlands
e-mail: h.h.smits@lumc.nl

Abstract

Immune homeostasis is essential to protect mucosal airway surfaces from unnecessary and damaging inflammation against inhaled harmless environmental antigens, such as allergens. However, in allergic individuals this protective homeostatic response seems to be absent. Innate cells that are part of the mononuclear phagocytic system (MPS) play an important role in these processes. Most of our knowledge on allergic immune responses comes from animal models or from peripheral blood immune responses in humans. Information on tissue-specific responses in humans is scarce, however allergen-specific immune responses are initiated locally and this information is therefore crucial for the development of novel therapies. In this study we performed mass-cytometry proteomics and single cell RNA sequencing on immune cells from nasal biopsies of allergic rhinitis subjects and non-allergic controls, before and three days after repeated nasal challenge with House Dust Mite allergen. Following challenge, patients displayed a clinical nasal response together with enhanced eosinophilia, a cardinal feature of allergic inflammation. Although clinically silent, we observed a distinct, local, innate immune response to allergen in non-allergic individuals, characterized by infiltration of HLA-DR^{low} CD14^{+} monocytes expressing anti-microbial genes (S100A8, S100A9, S100A12) as well as transcriptional activation in cDC2, including several inhibitory/tolerogenic genes (NR4A1, IL4I1, ANXA2, TIMP1). The innate response in allergic individuals indicated an inflammatory role for infiltrating HLA-DR^{hi} CD14^{+} monocytes, CD16^{+} monocytes, and CD1A^{+} cDC2 (ALOX15, CD1A, CCL17), in the development/maintenance of an allergic response. Future therapies should address those innate MPS populations, either enhancing or reducing their activity for the treatment of inflammatory airway disease.

Introduction

The (upper) airways form an intriguing organ, constantly exposed to potentially dangerous pathogens and harmless air-borne particles. Their mucosal surfaces consist of delicate soft tissue, vulnerable for inflammation-induced tissue damage. Therefore, it is of paramount importance to guard homeostasis by innate immune cells: driving anti-microbial responses to potential intruders and anti-inflammatory/regulatory responses to prevent unnecessary tissue damage. Allergic airway diseases, such as allergic rhinitis or allergic asthma, are typical examples of diseases where local immune homeostasis is disturbed.

Innate cells comprising the Mononuclear Phagocytic System (MPS) are key players in linking innate and adaptive immunity, as well as maintaining homeostasis and tissue integrity[1,2]. These include macrophages (MF), various subsets of monocytes (classical, intermediate and non-classical) and dendritic cells (DC); namely CD141$^+$ cDC1, CD1c$^+$ cDC2 and pDCs. Each cell type exhibits specific functions within the system to achieve these goals. MF are highly efficient phagocytes, clearing cellular debris and pathogens, and have the ability to induce inflammatory or anti-inflammatory responses[3,4]. Monocytes continuously enter the tissue from the circulation[5] and are involved in pathogen clearance, as well as wound healing. Monocytes can give rise to inflammatory monocyte-derived DC (mo-DC)[6] and MF, depending on the environment and phase of inflammation[7]. In contrast, DC are effective antigen presenters, activate naïve T cells and support their development into e.g. Th1 or Th17 cells in response to intracellular microorganisms or extracellular bacteria and fungi, respectively[8].

Exposure to essentially harmless and airborne environmental substances (including allergens) do not normally result in inflammatory responses. In the gut, this is achieved by induction of tolerance through molecules such as retinoid acid, TGFβ and IL-10, with subsequent induction of regulatory T cells[9]. Here, these molecules are promoted by low dose exposure to TLR ligands, specific microbial metabolites, or vitamin derivatives[10]. Local monocytes and MF can produce large quantities of anti-inflammatory cytokines such as IL-10, affecting many cell types in the tissue promoting immune regulation and homeostasis[11-13]. However, in allergic patients, Th2 cells, IgE-producing B cells and innate lymphoid cells (ILC)2 are induced in response to environmental antigens, such as allergens.

Much of our knowledge on these immune cells in humans has been derived from peripheral blood studies. Peripheral blood cells are usually easily accessible and in abundance or can be used as precursors to generate larger numbers, such as for mo-DC. In mucosal tissue, immune cells may differ from their peripheral blood counterparts due to the influence of the tissue environment and the proximity to foreign compounds, commensals, or pathogens. Nasal biopsies can provide valuable information on upper airway responses; however, this has been hampered by limited cell numbers obtained and technical limitations in immuno-profiling. Novel single cell analysis platforms, such as mass-cytometry and single-cell RNA sequencing, are finally providing key solutions to such roadblocks, vastly increasing the volume of data that can be obtained from relatively few cells. The recent technological advances have contributed to our understanding of epithelial and immune cell composition in the airways in both health and disease states[14,15], however these tools have not yet been applied to monitor airway cellular responses following environmental challenges, such as allergens.

To this end, we chose to study cellular responses in the context of allergic rhinitis, which affects the upper airways in response to allergens in patients but not in non-allergic individuals. We performed extensive, single cell proteome and transcriptome profiling of immune cells in nasal tissue of both allergic rhinitis and non-allergic subjects, before and after House Dust Mite (HDM) challenge, to identify the tissue cellular components of both non-allergic and allergic cellular responses to HDM. Our findings not only identify key players in airway inflammation but also elucidates a comprehensive blueprint of a ‘non-allergic’ response to allergens by MPS cells, which can be used to identify novel components capable of modulating the immune system for an appropriate response to allergens.

Results

Immune cell composition in nasal tissue.

Biopsies were obtained from non-allergic and allergic rhinitis subjects (**Table 1**) before and after three days of repeated HDM challenge (**Figure 1A**). Proteomic and transcriptomic profiles of the CD45$^+$ live cells were measured by mass-cytometry and single cell RNA-sequencing, respectively. In the first level of clustering of the proteomic data, 752,348 cells from 53 samples were divided into 13 lineages (**Figure 1B, S1**) and identified as CD8$^+$ T cells, CD8$^+$ MAIT cells, CD8$^-$ T cells (including CD4$^+$ T cells), TCRγδ cells, B cells, ILCs including NK cells, neutrophils, eosinophils, basophils, mast cells, monocytes, MF/DC, and an unidentified group of cells lacking clear cell lineage markers. In the following round of clustering, subpopulations of each lineage were generated. The transcriptomic data consisted of 46,238 cells from 75 samples, from which 26 cell clusters were generated (**Figure 1C, S2**). Major lineages including CD4$^+$ and CD8$^+$ T cells, B cells, NK cells, monocytes, DC and mast cells were identified based on established markers and enrichment analysis, corresponding with the populations detected in the mass-cytometry data (**Table S1**). Granulocyte populations, including neutrophils, eosinophils and basophils were not identified in the transcriptomic data. The process of cryopreservation of samples prior to scRNA-sequencing will have contributed to the loss of these cells. In addition, neutrophils and eosinophils contain high levels of RNAses, which can inhibit the reaction during cell capture and result in insufficient usable sequence reads. Difficulty in cell capture of neutrophils with the 10X Genomics Chromium platform has been acknowledged previously (10xgenomics.com).

Allergic rhinitis subjects display a type 2 phenotype.

Following the first nasal allergen challenge a symptom score was recorded to monitor the allergic response. Symptoms contributing to the score calculation included sneezing, itchy eyes, nasal congestion, and rhinorrhea. All allergic rhinitis subjects responded positively to HDM challenge, with a group average summed symptom score of 18 (range 9-28)[16]. All non-allergic subjects had symptom scores below 5, considered to be the threshold for a positive response to the allergen (**Table 1**). In allergic subjects, immunological indications of a type 2 phenotype were found (**Figure S3**). Higher levels of the high affinity IgE receptor FCER1A were detected in particular on mast cells of allergic subjects compared to non-allergic subjects (**Figure S3A**). Furthermore, pro-inflammatory, TH2A CD4$^+$ T cells[17] were detected in allergic subjects only (**Figure S3B**), and in response to allergen challenge, an influx of eosinophils and neutrophils was observed in allergic subjects only (**Figure S3C**). Finally, allergic subjects had a higher percentage of ILC2 compared to non-allergic subjects after allergen challenge (**Figure S3D**).

Composition of mononuclear phagocytic system (MPS) in nasal tissue.

As MPS cells play a dominant role in bridging innate and adaptive immunity, resulting in either tolerance or inflammation, we further explored the phenotype and response of the different MPS clusters to allergen challenge in both groups. In the single-cell transcriptomic data, MPS cells were distinguished from other immune cell populations based on expression of signature markers LYZ, CST3, AIF1, LST1, and HLA-DRA. Top differentially expressed genes of the individual MPS clusters were then identified (**Figure 2A, S4, Table S2**), and each cluster was annotated based on the expression of established markers (**Figure S5**) and Enrichr gene set enrichment analysis with the Human Gene Atlas and ARCHS4 Tissues databases (**Figure 2B**). To further support cluster annotation, average gene expression of each cluster was calculated and plotted along with cell signature profiles of MPS cells from previous transcriptomic studies (**Figure 2C**). The profiles chosen were derived from (single cell) RNA sequencing studies of peripheral blood and tissue DC, MF and monocytes[15,18-22]. Cluster 4, 13 and 23 display a transcript profile consistent with monocytes. Cluster 4 corresponds primarily with CD14$^+$ monocytes, cluster 13 with CD16$^+$ monocytes and cluster 23 with monocytes with a cytotoxic profile, previously described by Villani *et al.*[18], along with CD3 expression (**Figure 2A, 2C, Table S2**) which may be evidence of doublet forming. These cells (cluster 4, 13 and 23) clustered separately from DC (cluster 5, 15 and 22) and expressed established monocyte markers S100A8, S100A9, FCN1 and MNDA. Cluster 18 could be identified as a macrophage population expressing APOC1, APOE and MRC1, along with components of both M1 and M2 transcript profiles **(Figure 2C)**, previously described in alveolar MF[20]. We further identified CLEC4C$^+$ pDC (cluster 15), CLEC9A$^+$ cDC1 (cluster 22) and CLEC10A$^+$, CD1C$^+$ cDC2 (cluster 5) populations. Cluster 5 gene expression profile correlated with that of several distinct cell types including cDC2, Langerhans cells and 'AS' DC[18,23] (**Figure 2A, Table S2**).

In the mass-spectrometry proteomic data, MPS cells were identified at the first level of clustering as separate lineages of HLA-DR$^+$ cells (**Figure 3A**) expressing MPS cell markers such as CD11c, CD14, CD141 or CD123 (pDC), and lacking B cell marker CD19 (**Figure 1B**). The next level of clustering resulted in a total of 23 MPS cell subpopulations. Based on the markers expressed, populations of CD14$^+$ monocytes, CD16$^+$ monocytes, CD34$^+$ progenitor cells, CD206$^+$ MF, CD141$^+$ cDC1s, FCER1A$^+$ cDC2s and CD123$^+$ pDCs could be identified (**Figure 3B**). Overall, the populations identified in the proteomic data corresponded well with the major populations identified in the transcriptomic measurements, i.e. CD14$^+$ monocytes, CD16$^+$ monocytes, pDC, cDC1, MF and multiple cDC2 clusters (**Figure 3C**).

Recruitment of different monocyte populations in response to allergen challenge.
In response to allergen challenge, we observed an increase in the percentage of CD14$^+$ monocytes in both non-allergic and allergic subjects. This was confirmed in both proteomic (**Figure 4A,** clusters P4, P5, P10) and transcriptomic data (**Figure 4B,** cluster T4). In allergic subjects the percentage of an immature monocyte population, expressing intermediate levels of HLA-DR and low levels of CD34, increased upon allergen provocation (cluster P4; **Figure 3B**). In non-allergic individuals, an increase in two other immature cell populations was observed, one of which (cluster P5) displayed a progenitor monocyte phenotype, expressing low levels of HLA-DR and intermediate levels of CD34, but lacking pan markers CD11c and CD14 (**Figure 3B**). The other immature population (cluster P10) lacked HLA-DR and expressed low levels of CD11c and CD14 (**Figure 3B**). It should be noted that, while it did not reach significance threshold, a small increase in these populations was also detected in allergic subjects ($p<0.1$; **Figure 4A**). These changes are in line with the increase in percentage of CD14$^+$ monocytes in both cohorts measured from the transcriptomic data (**Figure 4B**).

Further clustering of the CD14$^+$ monocytes in the transcriptomic data (cluster T4) revealed five sub-clusters (**Figure 4C, Table S3**). The sub-clusters can be divided into HLA-DRA^{hi} and HLA-DRA^{low} monocytes (**Figure 4D and 4E**). Similar to the proteomic data, the frequency of cells in the HLA-DR^{low} sub-clusters (0,2,3) and HLA-DR^{hi} sub-clusters (1,4) increased in allergic subjects, whereas only the frequency of cells in the HLA-DRA^{low} sub-clusters (0,2,3) increased in non-allergic subjects after challenge (**Figure 4F**). Due to low cell numbers, we were unable to determine which of the individual sub-clusters increased in frequency. However, the proportions of each sub-cluster within the CD14$^+$ monocytes suggest that in non-allergic subjects after challenge sub-cluster 2 and 3 make up a larger portion of the CD14$^+$ monocytes compared to before challenge, resulting in relatively fewer HLA-DR^{hi} monocytes (sub-cluster 1,4) (**Figure 4G**). This is also represented by a decrease in ISG15 and IFITM3 gene expression, which are among the top gene markers of sub-cluster 1 and 4, in CD14$^+$ monocytes of non-allergic subjects **(Table S4)**. In allergic subjects primarily the proportion of cluster 0 of the HLA-DR^{low} monocytes increased after challenge. Further analysis with larger cell numbers are needed to confirm these findings (**Figure 4F**).

Sub-cluster 1 and 4 express higher levels of HLA-related and IFN-related genes compared to the other monocyte clusters, corresponding with antigen presentation, cell activation and differentiation and response to stimulus processes **(Figure S6)**, suggesting a pro-inflammatory role. Within these clusters FCGR3A expressing cells are also present, which may represent CD14+CD16+ monocytes **(Figure 4H)**. In addition, sub-cluster 4 expressed genes related to cell adhesion, migration, proliferation, regulation of ERK1/2 cascade and Th2 cytokine signaling (**Figure S6, Table S3**) along with genes consistent with a MF transcript profile (MRC1, APOC1) in a portion of cells. Sub-cluster 0, 2 and 3 express lower levels of HLA-DR, but higher levels of anti-microbial response genes S100A8 and S100A9 (**Figure 4I**). However, S100A9 has also been associated with an immunoregulatory function in Mo-MF involving ROS and possibly IL-10 production[24]. Sub-cluster 2 expressed the lowest levels of HLA-DRA along with the highest levels of S100A8, S100A9 and S100A12 compared to all other monocyte sub-clusters (**Figure 4D, 4I**). This gene profile is comparable to that of myeloid-derived suppressor cells[25], which play a role in immunosuppression in cancer and chronic inflammatory conditions[26-28], but have also been detected in peripheral blood of non-allergic individuals at low frequencies[29]. Sub-cluster 3 is distinguished by gene expression related to RNA translation (RLP36A, RABPC1, EIF3E, EIF3M, ZFP36L2; **Figure S6 and Table S3**), while cells of sub-cluster 0, which is the primary CD14+, HLA-DR^{low} sub-cluster to increase in allergic individuals, express higher levels of CRIP1 (cysteine-

rich intestinal protein). CRIP1 is highly expressed in immune cells and belongs to a family of LIM domain proteins[30]. Interestingly, overexpression of CRIP1 in transgenic mice resulted in a cytokine pattern favouring Th2 cytokines, suggesting a 'pro-allergic' role for this protein in T cell differentiation[31,32].

In addition to CD14^{+} monocytes, a significant increase in the frequency of CD16^{+} monocytes was observed in the allergic subjects only after allergen provocation. This was observed in both the proteomic (**Figure 5A**) and transcriptomic (**Figure 5B**) data sets. Combined, these results show an increase in frequency of HLA-DR^{low} CD14^{+} monocytes with an anti-microbial/regulatory signature in both subject groups but in particular in non-allergic subjects in response to allergen challenge, and an additional increase in HLA-DR^{hi} CD14^{+} monocytes and CD16^{+} monocytes in allergic subjects only, favouring an antigen presenting role.

Differences in the balance between effector and anti-inflammatory cDC2 in allergic and non-allergic subjects

In both the proteomic and transcriptomic data, multiple cell types within the original cDC2 cluster were identified. In the proteomic data cDC2 clusters (1,8,11/23) could be distinguished from CD14+/CD206+ DC (16,12, 23), CD5+ CD123+ DC (17) and CD163+ CD14+ CD16+ macrophages (9) (**Figure 3B**). In the transcriptomic data, additional clustering of this population (cluster T5) resulted in seven distinct clusters (**Figure 6A**) which, to an extent, could be aligned with recently identified cell types (**Figure 6B, 6C**) and some of the proteomic cDC2 clusters (**Figure 6D, S6**), and further characterised by genes for cell phenotype and function from the top differentially expressed genes of each cluster (**Figure 6E, 6F**). The majority of the cDC2 sub-clusters (cluster 0-3 and 6) could be identified as cDC2 cells based on their expression of CD1C, FCER1A and/or CLEC10A, with two additional clusters (cluster 4 and 5) that lacked these markers (**Figure 6B, 6C**).

Recently, extensive analysis of cDC2 phenotypes in tissue in both humans and mice by Brown *et al*.[33] resulted in the identification of effector/inflammatory cDC2 termed cDC2B and anti-inflammatory cDC2 termed cDC2A. Compared to cDC2B, cDC2A lack expression of CLEC10A, PSAP, NPC2 and CEBP transcription factors, express lower levels of CD1c and FCER1A and higher levels of RUNX3, LTB, AREG, IDO1, CD300a, IL22RA2 and CLEC4A. In culture, cDC2A stimulated with TLR7 ligands showed reduced production of pro-inflammatory cytokines IL-6 and TNFa compared to cDC2B. Furthermore, murine cDC2A had reduced ability to polarize naive T cells toward IFNγ or IL-17A production compared to their cDC2B counterparts, while both subsets exhibited a similar capacity to support Foxp3+ T cell differentiation. cDC2A are not present in peripheral blood but are enriched in mucosal areas indicating that they may be dependent on microbiota-derived signals[33]. We found sub-cluster 2 and 6 to contain cells that express markers corresponding with a cDC2A profile, based primarily on CD1C, CCR6, LTB, RUNX3, IL22RA2 and a lack of or reduced expression of CLEC10A, PSAP and CD86 (**Figure 6B, 6C**). However, it should be noted that some of the cDC2A markers defined by Brown *et al.*[33] were absent in these clusters, including CLEC4A, AREG and NR4A3 which may be due to differences in the source of cells (airways versus spleen), or due to effects of cell handling. Sub-cluster 6 additionally expressed genes consistent with Gene Ontology terms related to mitosis (**Figure S7**), representing a 'mitotic cDC2A' subset, which was also described by Brown *et al.*[33] The remaining cDC2 populations, sub-clusters 0, 1 and 3, expressed cDC2B markers (CLEC10A, CD1C, FCER1A), but each expressed a distinct profile (**Figure 6E, 6F**). Sub-cluster 1 contained cells expressing a monocyte-like profile FCN1, SELL, S100A8, S100A9, which corresponded to mo-DC or the recently described inflammatory DC3 population by Villani *et al.* [18,34,35]. In contrast, sub-cluster 3 expressed higher levels of the regulatory/inhibitory genes FCER1A, FTL, FCGR2B, RGS2[7,36-39] and VSIG4[40,41] along with MAPkinase signaling pathway genes (FOS, FOSB, JUN, JUNB, DUSP1) **(Figure 6E, Table S5)**, which may represent the 'non-inflammatory' FCGR2B cDC2 described by Villani *et al*.[18], but are also related to cellular stress response **(Figure S7)**. Sub-cluster 0 was distinguished by its expression of effector DC markers (NMES1 IFITM3, NPC2)[33,42], and expressed higher levels of genes related to cell activation, defence response and antigen processing and presentation compared to the other sub-clusters (**Figure S7, Table S5**). Sub-cluster 0 also contained cells expressing CD1A, which is similar to cluster 11 and 23 in the proteomic data (**Figure 3B, S6**). In the lung, CD1a^{+} "pulmonary DC" have been described as potent T cell stimulators[2,43,44]. We found a higher percentage of this cDC2 cluster in allergic subjects compared to non-allergic subjects at baseline, detected in both the proteomic and

transcriptomic data (**Figure 6G, 6H, 6I**). In contrast, the percentage of cluster 8 in the proteomic data, containing FceRI^{low}, CCR6^{+} HLA-DR^{low} cells similar to cells within the anti-inflammatory cDC2A sub-cluster 2 and 6 of the transcriptomic data, is higher in non-allergic subjects compared to allergic subjects (**Figure 6J**). These findings indicate the presence of multiple, distinct cDC2 populations and dominance of effector (CD1a^{+}) cDC2 cells in allergic subjects, while more regulatory subtypes seem to be overrepresented within the non-allergic individuals. Interestingly, following challenge, a decrease was detected in the percentage of CD1a^{+} cDC2 and CD14+ DC in allergic subjects in the proteomic data, which might be due to migration of these cells (**Figure 6K**).

Differential gene expression analysis of all cDC2 cells (cluster T5 of MPS cells), between before and after challenge show upregulation of ALOX15, CD1B and CD1E in allergic subjects but not non-allergic subjects (**Figure 6L, 6M, Table S4**). Cells predominantly expressing these genes belonged to CD1a^{+} cells (sub-cluster 0) within the cDC2 cells. ALOX15 is induced by Th2 cytokines IL-4 and IL-13, therefore the upregulation of this gene suggests local IL-4/IL-13 release in response to allergen challenge in the allergic subjects. CD1 genes belong to the lipid antigen presentation pathway and are associated with DC maturation. Upregulation of these genes can point at an increased capacity to present antigens to T cells following allergen encounter. CKB is primarily expressed in non-classical monocytes and might indicate the differentiation of these cells into (mo-)DC[45], following infiltration into the nasal tissue. Further analysis of ALOX15 expressing cells, revealed these cells expressed higher levels of CD1 (CD1A, CD1B, CD1D, CD1E), and additional IL-4 or STAT6 inducible genes (CCL17, LIPA, FABP5, DNASE1L3, SPINT2) compared to ALOX15 negative cells of cluster T5 (**Figure 6N**).

Overall, more genes were upregulated in cDC2 cells of non-allergic subjects compared to allergic subjects in response to allergen. These genes were related to the GO term 'regulated exocytosis', and individual genes related to cytoskeleton/membrane remodeling, cell metabolism, cell survival and mediator secretion. Furthermore several genes were shown to have anti-inflammatory or regulatory functions, or to be expressed in tolerogenic DC (NR4A1, IL4I1, FTH1, ANXA2, TIMP1)[46-52], and several of these genes have also been shown to be up-regulated in response to LPS[48,53-55].

CCR7+ DC and Pre-DC identified in the nasal cDC2 compartment

Within the cDC2 cells, a small sub-cluster (106 cells) was identified as a mature DC population (sub-cluster 5; **Figure S7, Table S5**), expressing CCR7, CD83 and LAMP3, but did not correspond with any particular DC subset based on known markers. CCR7 serves as a homing receptor for cells migrating towards the lymph nodes and is upregulated upon maturation. However, genes related to a regulatory function (SAMSM1, IL4I1, RELB, IDO1, IL7R) with potential for Treg induction were also among the top markers for this subset (**Figure 6E, 6F**). In homeostatic conditions, these cells have been shown to induce self-antigen-specific regulatory T cells to maintain peripheral tolerance. In cancer, this regulatory function has been shown to be exploited by tumor cells to facilitate tumor evasion[56]. An equivalent CCR7^{+} DC cluster in the proteome dataset was not detected (**Figure 3B**), which might be explained by differences between transcript and protein levels. Indeed, a similar discrepancy has been observed in mono-mac-1 cells, where upregulation of CCR7 mRNA did not result in increased protein expression[57]. IL7R (CD127) also served as a distinguishing marker for CCR7^{+} DC in the transcript data and was detected on a small portion of cluster P23 in the proteomic data, and might point at the same population (**Figure S8**). To our knowledge this is the first report of this population being present in the upper airways and, due to its unique profile, it may provide a potential target for modulation of the immune response.
Sub-cluster 4 was identified as the recently described AS-DC or pre-DC[18,23], based on AXL, DAB2, PPP1R14A and LILRA4 expression (**Figure 6B, 6C**). This cluster aligned with cluster P17 in the proteomic data, positioned between pDCs and cDC2 populations and expressing CD123, CD5 and CD11c (**Figure 3B, S6, 6D**). Pre-DC are potent T cell stimulators and have been found to infiltrate the airways within 8 hours in response to LPS inhalation[58], however the percentage of this cell population within all mononuclear cells did not differ between groups or in response to allergen challenge in this study.

MF gene upregulation in response to allergen challenge in non-allergic subjects.

In response to allergen challenge in non-allergic subjects, a higher percentage of MF (cluster T18) expressed Major Vault Protein (MVP) along with SRGN and LIMS1 **(Table S4)**. MVP interacts with TRAF6, inhibiting its activity and subsequent NF-kB signalling, thereby suppressing macrophage

inflammation. This has been shown to be a negative regulator of obesity and atherosclerosis by suppressing inflammation in mice[59], and down regulation of TLR4/TRAF6/NF-kB pathway through other means has been shown to attenuate murine allergic rhinitis[60]. NF-kB is a transcription factor required for the induction of inflammatory genes, including TNFα, IL-1B, IL-6 and IL-12 in MF, which can contribute to the development of allergic airway inflammation[61].

Discussion

Mucosal surfaces in the upper airways are constantly challenged by pathogens and foreign particles but should maintain immune homeostasis to protect against unnecessary and chronic inflammation. We here performed a comprehensive single cell proteome and transcriptome analysis on nasal tissue biopsies following controlled allergen challenge in allergic and non-allergic individuals to obtain deeper insights into these processes and the role of innate immune cells.

To our knowledge this is the largest number of subjects in one single cell RNA sequencing dataset to date, providing a comprehensive overview of innate immune cells present in nasal tissue in both non-allergic and allergic subjects. Within the CD14^{+} monocyte population we identified five sub-clusters, which could be grouped into HLA-DR^{hi} and HLA-DR^{low} populations, which was also detected in the proteomic data. In non-allergic individuals, only HLA-DR^{low} CD14^{+} monocytes significantly increased in frequency in the nasal tissue in response to allergen, whereas in allergic subjects the frequency of HLA-DR^{hi} CD14^{+} monocytes and CD16^{+} monocytes also significantly increased. Furthermore, one of the HLA-DR^{low} CD14^{+} monocyte clusters we identified to increase in non-allergic subjects, expressed a gene profile similar to that of myeloid-derived suppressor cells, consisting of high levels of anti-microbial S100A8/9/12 genes[59]. These cells have been shown to accumulate in cancer and suppress T cell responses, however their precise role in asthma or allergy is not clear. The striking combination of anti-microbial and regulatory genes can also be found in mo-MF: here, expression of S100A9 induced an immunoregulatory function involving ROS and possibly IL-10 production[24]. This MF phenotype can also be enhanced through stimulation with butyrate[62], a short chain fatty acid (SCFA) produced by gut microbiota. Butyrate has immunoregulatory effects and induces tolerance to microbial communities in the gut, but it is also found systemically and can act distally in the (upper) airways influencing local immune cells[63,64]. Depending on the composition of the airway microbiota, SCFA can be increasingly metabolized limiting their bioavailability[65]. Although we did not determine the nasal microbiota composition, differences between allergic and non-allergic individuals have been demonstrated in other studies (reviewed in[66]). It is tempting to suggest that those – and/or the bioavailability of microbial metabolites - may have influenced the immune status of local monocyte populations in our study participants.

In contrast to HLA-DR^{low} monocytes, CD14^{+}CD16^{-} and CD14^{+}CD16^{+} monocytes expressing high levels of HLA-DR are considered pro-inflammatory, and their recruitment has been implicated in various inflammatory diseases[67,68]. CD16^{+} CD14^{-} monocytes have been termed patrolling monocytes and are recruited to areas of inflammation to assist in tissue repair. However, CD16^{+} monocytes have been shown to differentiate into mo-DCs, with migratory abilities[69] that produce TNFa[45] or induce higher levels of IL-4 production from CD4 T cells compared to CD16^{-} monocytes[69-71]. In allergic disease, this may perpetuate the Th2 type response.

In the cDC2 compartment we found an effector (CD1a^{+}) cDC2 subpopulation to dominate in allergic subjects at baseline, and these cells in particular were found to respond to allergen challenge in allergic individuals. This population is one of the cDC2B clusters we identified, which has been defined as pro-inflammatory by Brown *et al*. Furthermore, previous studies of the nasal mucosa have found elevated numbers of mature CD1a+ DC in allergic rhinitis compared to non-allergic individuals[72,73]. In contrast, in non-allergic individuals the cDC2 subpopulations are more balanced, including a previously described anti-inflammatory cDC2A population and FCGR2B^{+} cDC2 cells[18,33]. cDC2A have been described as anti-inflammatory T-bet+ cDC2, induced by IFNγ however, a recent study of migratory CD11b+ DC in mice revealed upregulation of T-bet, in response to TNFα,, which was induced through HDM and LPS stimulation. This, in turn, promoted T-bet expression in T cells and prevented a Th2 response from being mounted towards the allergen[74]. Further investigation of the population we have identified would be required to ascertain how they respond to stimuli, however either an anti-inflammatory or Th1 response would be beneficial in preventing or reducing a Th2 response towards allergens. Interestingly, the cDC2A and cDC2B cells, as they have been described, do not arise from distinct progenitor cells and likely acquire their specific transcriptional profiles through environmental cues[33]. In this case, variations in microbiota composition in the airways may influence cDC2 differentiation and, ultimately, the balance between the different cDC2 subtypes.

FCGR2B cDC2 represent a separate cluster that is distinguished by higher expression of several anti-inflammatory/regulatory markers (FCER1A, FCGR2B, FTL, VSIG4). This population also expressed higher levels of MAPkinase signalling pathway genes (FOS, JUN) which may indicate cellular proliferation, differentiation or survival in response to inflammatory cytokines or stress. Up-regulation of these genes, however, may also have been induced in response to collagenase treatment of the tissue biopsies[75]. The precise function of these cells is not clear; however their expression profile indicates that they may have a regulatory role, which may be relevant during inflammation. Furthermore, Villani *et al*.[18] made the distinction between 'non-inflammatory' FCGR2B$^+$ DC2 and 'inflammatory' FCGR2B$^-$ CD163$^+$ CD36$^+$ DC3.
In response to challenge in non-allergic individuals, genes are upregulated in cDC2 that relate to regulation of exocytosis, along with several genes that have been associated with or are markers of regulatory or anti-inflammatory functions. This indicates that there is indeed an immune response to allergen challenge in non-allergic subjects, but interestingly the cDC2 response seems to also include an immunoregulatory element. As this subset is relatively new, more research needs to be established to get more insight in its functional capacities and its potential to prevent or reduce allergic immune responses.

Similar to our findings, a previous study of experimentally induced airway inflammation with grass and tree pollen showed a rapid influx of CD14$^+$ HLA-DR$^+$ monocytes in the nasal tissue of allergic rhinitis subjects. This was detectable at 3 days and as early as 12 hours after allergen challenge[76], followed by recruitment of Th2 cells and eosinophils. Transcriptome analysis of CD45$^+$HLA-DR$^+$ cells within nasal biopsies after an 8-day allergen challenge revealed upregulation of genes regulated by IL-4 and or IL-13, including ALOX15, CD1A and CD1B. The origin of these transcripts (monocytes, cDC or pDC) could not be identified in the study due to low cell numbers, however we have now determined these transcripts to be derived from CD1A$^+$ cDC2 cells (within sub-cluster 0 of cDC2 cells) expressing CCL17 and other IL-4 inducible genes. Furthermore, our data shows this expression profile to be present in resident cDC2, prior to an increase in the frequency of dendritic cells in the airways, which several studies have shown to occur after 7-8 days of repeated challenge[76-78]. The origin of the accumulating DCs after pro-longed, repeated allergen challenge in other studies is not clear, however whether these cells are recruited from the bone marrow or are derived from previously infiltrated monocytes[79].

In contrast to our findings, an increase in monocytes of non-allergic subjects in response to pollen allergen challenge was not detected by Gracia *et al.*[76] However, this may be due to the composition and the type of the allergen extract used. In our study, controlled allergen challenge was performed with a total HDM extract from which endotoxin was not depleted, representing the allergen composition encountered in non-experimental, everyday settings. LPS inhalation has been shown to induce neutrophil, CD14^{++} CD16$^-$ monocyte and CD1c$^+$ DC recruitment to the airways in non-allergic individuals. Additionally, upon LPS challenge, monocytes expressed lower levels of antigen presenting genes, higher levels of LPS-response genes (e.g. IL1A, IL1B), and retained S100A8/9 and SELL expression in comparison to steady state, which would be similar to infiltrating HLA-DR^{low} monocytes. LPS inhalation also induced IL1B expression in recruited CD1c$^+$ DC, which we observed in DCs of non-allergic individuals after allergen challenge[58]. Furthermore, severe systemic inflammation, as observed in sepsis patients, is linked to a decreased expression of HLA-DR in monocytes[80-82]. It is noteworthy that more rural environmental conditions with increased microbial exposure, such as living on family dairy farms, was associated with decreased HLA-DR expression on circulating monocytes compared to the non-farmer community. Expression of both innate defense and immunoregulatory genes were increased in children raised on farms, an environment associated with protection against the development of allergic airway inflammation[83]. Supporting this, endotoxin exposure (in farm dust) in mice also offers comparable protection[83-85]. This suggests that regular microbial exposure, linked to protection for the development of allergic disease, may contribute to maintenance of mucosal homeostasis through priming of local innate immune cells. Although these findings may partially explain the changes, we observed in non-allergic individuals following HDM challenge, the question remains why nasal endotoxin exposure (in the allergen extract) did not induce a similar immune response in allergic subjects. A recent paper suggests that this might be related to a modified innate response as a consequence of epigenetic programming called 'trained innate immunity'[86].

Despite the large number of subjects included in this transcriptomic data, there are specific limitations to this part of the study. The cell numbers obtained varied per sample and for a portion

of the samples was too low to contribute to smaller (sub)clusters, including MF, which made it difficult to identify changes or differentially expressed genes between groups or conditions in these populations. The transcriptomic data was derived from cells which had been released from tissue through enzyme digestion and then cryopreserved, before being thawed and FACS sorted. This allowed for all cells to be captured in only five carefully assigned batches, however, background signal or noise may have increased due to cell handling, which possibly led to the loss of detection of subtle changes in differentially expressed genes. Finally, although we were able to align our cell types with those described in previous studies and thereby extrapolate as to the functional properties of those cell types, further functional analysis of the cells is required to definitively identify their role in tolerance and allergic disease and how this can be targeted in novel treatments of individuals with aero-allergens.

Collectively, our data indicates a distinct, local, innate immune response to allergen in non-allergic individuals, characterized by infiltration of HLA-DR^{low} CD14^{+} monocytes and transcriptional activation of cDC2, including upregulation of tolerogenic genes. The response in allergic individuals indicates a role for infiltrating HLA-DR^{hi} CD14^{+} monocytes, CD16^{+} monocytes, and ALOX15 upregulation in CD1A^{+} cDC2, in the development of maintenance of an allergic response. Future therapies should be tailored towards those innate populations, either enhancing or reducing their activity for the treatment of allergic airway disease.

Methods

Study design and sample collection

Adult subjects sensitized to house dust mite (HDM) who fulfilled the ARIA criteria[87] for moderate to severe persistent allergic rhinitis and non-allergic subjects, without sensitization to inhalant allergens, and without clinical features of allergic rhinitis were included in the study. Allergic subjects had a history of perennial rhinitis symptoms with or without conjunctivitis, and were skin prick test positive to HDM extract (Der. Pteronyssinus, ALK-Abello, Denmark) (skin wheal area ≥ 0.4 HEP, corresponding with the internationally accepted wheal diameter of ≥ 3 mm). Non-allergic subjects had no history of allergic rhinitis and were SPT negative to HDM, birch pollen, grass pollen, cat and dog or other animals with which they were in daily contact with. Exclusion criteria consisted of pregnancy, nasal polyps and anatomical or other disorders of the nose. In total 30 allergic subjects with and 27 non-allergic subjects were recruited (**Table 1**).

Nasal Allergen Provocation

Nasal allergen provocations with HDM extract (ALK-Abello) were performed according to the protocol shown in Figure 1A, as described previously[88-90]. Provocations were performed once a day on three consecutive days. Nasal corticosteroids and antihistamines were withdrawn 3 weeks and 3 days respectively before the provocation. Provocations were performed in the absence of total nasal obstruction or infection as assessed by rhinoscopy. The nasal provocation on the first day was performed with 3 increasing doses of allergen extract (100,1000,10000 BU/ml) into both nostrils at 10-minute intervals after sham challenge with PBS containing human serum albumin 0.03% and benzalkonium chloride 0.05%. (ALK Abelló). The nasal response was assessed with a score system according to Lebel[16]. The second and third challenge into one nostril were performed with PBS and HDM 10000 BU/ml only. PBS and the allergen extract were sprayed into the nostrils with a nasal pump spray delivering a fixed dose of 0.125 ml solution. Nasal provocations were performed out of pollen season between September 2017 and February 2018.

Nasal biopsies

Biopsies were taken twice: once before the allergen provocations from one nostril and once one day after the third allergen provocation from the other nostril. Three 2mm^2 biopsy samples were taken from the inferior turbinate. Beforehand, the nasal mucosa was anaesthetized by inserting 3 pieces of cotton wool on the mucosa soaked in 5% cocaine hydrochloride that was inserted onto the mucosa. 15 Minutes were allowed for the local anaesthetic to take effect. Following this, biopsy samples were taken using a specially developed Gerritsma biopsy forceps (Phoenix Surgical Instruments Ltd, Hertfordshire, UK). Haemostasis was achieved by packing the nose with cotton wool balls soaked in 0.5mL of 1:1000 adrenalin. These were removed after 15 minutes and the nose was then examined for sites of bleeding, if present, areas were cauterised with a bipolar electrocoagulation (Erbe Surgical Systems, Marietta, Georgia, USA). The patient was observed for a further 15 minutes and cauterisation was performed again if necessary.

Ethical Statement

All subjects gave written informed consent and research was conducted in compliance with all relevant ethical regulations. Ethical approval was given by Erasmus Medical Centre Ethics Committee in Rotterdam (MEC2016-560).

Nasal biopsy digestion

At each visit, before and after allergen challenge, three individual nasal biopsies were taken and stored in 5mL of cold 10% FCS IMDM for no longer than 1 hour. The biopsies were then finely cut using a sterile scalpel and digested in 10% FCS IMDM with Liberase TL (125 µg/mL, Sigma-Aldrich, MO, USA) and DNAse I (100 µg/mL, Sigma-Aldrich) overnight at 4°C. After digestion, an equal volume of FCS was added and the suspension was vortexed for 30 seconds. The biopsies were then pressed through a 100µm filter, rinsed thoroughly with IMDM and filtered over a 70µm filter. Cells were spun down for 10 minutes at 400 x g followed by red blood cell lysis with an osmotic lysis buffer (eBioscience). Cells were then resuspended in RPMI 1640 and counted. From each sample, 1x10^5 cells were removed and cryopreserved, as described in the PBMC isolation section, for single cell RNA sequencing at a later date. The remaining cells were spun down for 10 minutes at 400 x g and resuspended in staining buffer (Fluidigm, CA, USA) for mass cytometry staining with metal-conjugated antibodies.

Mass Cytometry Measurements and Analysis

Antibody-metal conjugates **(Table S1)** were purchased from Fluidigm or conjugated using 100 µg of purified antibody and the Maxpar X8 Antibody Labelling kit (Fluidigm). Conjugated antibodies were stored at 4°C in Antibody Stabilizer PBS (Candor Bioscience, GmbH, Wangen, Germany). All antibodies were titrated prior to use. Cells were stained with metal conjugated antibodies for mass cytometry according to the Maxpar Surface Staining protocol V2. Briefly, cells were stained with 1 µM intercalator Rh-103 (Fluidigm) for 15 minutes, washed and incubated for 10 minutes with TruStain FcX-receptor block (Biolegend) prior to a 45-minute incubation period with the antibody cocktail **(Table S1)**. Cells were washed twice with staining buffer and incubated for one hour with 1 mL of 1000x diluted 125 µM Cell-ID intercalator-Ir191/Ir193 (Fluidigm) to stain DNA for cell identification. Cells were then washed three times with staining buffer and twice with deionized H_2O. Finally, EQ Four Element Calibration Beads were added for normalization and cells were acquired on a Helios 2 mass cytometer (DVS Sciences). In addition to the metals included in the panel, channels to detect intercalators (103Rh, 193IR, 193IR), calibration beads (140Ce, 151Eu, 153Eu, 165Ho and 175Lu) and contamination (133Cs, 138Ba, 206Pb) were included during measuring. After data acquisition, the files were normalized with the reference EQ passport P13H2302 and where applicable concatenated. The median biopsy yield measure by mass-cytometry was 6,76 x 10^4 cells (IQR: 2,46 x 10^4 to 9,72 x 10^4) per sample, of which 80,6% (median) were stromal cells. Viable, single CD45+ cells were pre-gated according to previously a described gating strategy[91] **(Figure S9)** and exported as new FCS files with Flowjo V10 for Mac (FlowJo LLC, Ashland, OR, USA). Data was transformed with hyperbolic arcsinh using a cofactor of 5 and distinct cell clusters were identified with Hierarchical Stochastic Neighbor Embedding (HSNE) in Cytosplore (https://www.cytosplore.org/) **(Figure S1)**. Clustering was performed in two levels, once to determine the lineages present and another on the identified lineages. The second level of clustering on the MPS lineage was performed without the FceRI marker, as inclusion of this marker lead to additional clusters solely based on FceRI expression, which differed significantly between the non-allergic and allergic cohort (**Figure S3A).** The original MPS cluster 11 could be further split into two populations (cluster 11 and 23) which differed in CD206 expression **(Figure 3B)**. Cytosplore output was analysed with the 'Cytofast' package (rdrr.io/github/KoenAStam/cytofast)[92] in RStudio (Rstudio, Inc., Boston, MA, USA, www.rstudio.com), to produce heatmaps, scatterplots of subset abundance and histograms of the median signal intensity distribution of markers. Cell numbers were normalized to the total number of CD45+ cells or mononuclear cells (CD45+ cells with granulocyte numbers removed, in order to compare to findings from the transcriptomic data) for each subject to correct for varying biopsy yields.

Normalized frequencies were then compared between non-allergic and allergic subjects, and between before and after allergen challenge for each of the lineages and subpopulations. Two-tailed, nonparametric statistical tests were used throughout the study. The Mann-Whitney was used to compare subset abundance between groups. The Wilcoxon test was applied to compare pre-and post challenge samples. Correcting for multiple testing was not performed. P values <0.05 were considered statistically significant.

Single cell RNA sequencing

Cryopreserved cells from digested nasal biopsies were thawed in pre-warmed 10% FCS RPMI 1640 and spun down at 300 x g for 10 minutes. Cells were resuspended in Cell Staining Buffer (Biolegend) containing TruStain FcX-receptor block (Biolegend) and incubated for 10 minutes on ice. TotalSeq cell hashing antibodies were then added following manufacturers recommendations, along with anti-CD45-APC (HI30, Biolegend). After a 15 minute incubation period on ice, the cells were washed with staining buffer and spun down at 300 x g for 10 minutes at 4°C. Supernatant was removed, cells were resuspended in staining buffer, and all samples were combined before adding 7AAD for exclusion of dead cells. Live, single CD45+ cells were sorted on a FACSAriaIII (BD Biosciences) into eppendorfs containing 0,04% BSA PBS. Cells were delivered to the Leiden Genome Technology Centre for single cell sequencing on the 10X Genomics Chromium system. A maximum of 30000 cells, from 15 barcoded samples, were encapsulated in each individual run, for a total of 5 runs **(Figure S10)**. Cells were loaded according to the standard protocol of the Chromium single cell 3' kit at a maximum concentration of 1000 cells/µl. Sequencing was performed on two lanes of an Illumina Hiseq 4000 to obtain coverage of at least 30000 reads/cell.

Transcriptomic data mapping cells to subjects

Each barcode log-counts distribution over all cells of a single run followed a bimodal shape with well separable peaks. The high-count peak was interpreted as the signal for a particular barcoded donor. For each sample a two-component gaussian mixture model was fitted and a cell was assigned to a donor when it was at least 3 times more likely to be explained by the donor's high-count peak than by the donor's noise low-count peak **(Figure S11).** The majority of the cells were assigned to a single donor only **(Figure S12)**. Cells that could not be assigned to a single donor were excluded from further analyses.

The barcode-based assignment was validated by investigating concordance between genotypes of samples assigned to the same donor but sequenced in different runs. In the pileup of pooled, aligned reads from all runs, genomic positions (SNPs) likely to differ between donors were identified. At each such position and separately in each cell we generated the count of transcripts with the reference base and count of transcripts with the alternative base(s). Cumulated positional counts of cells were assigned to the same sample and sample genotypes were called. Concordances were calculated for all sample pairs, and clear separation was observed for concordances expected to belong to the same donor vs. different donors **(Figure S13 and S14)**. Positional counts of cells assigned to the same donor across multiple runs were cumulated and genotypes of all donors were called. A genotype-based donor assignment was then performed, by identifying the most likely genotype for each cell. Cells that were consistently assigned to the same donor by barcode-based and genotype-based methods were selected for further analysis **(Figure S15)**.

Single cell RNA sequencing analysis

The five demultiplexed gene expression matrices were imported in R package Seurat v3, retaining only genes expressed in at least three cells, and merged into a combined Seurat object. Cells with less than 200 or more than 4000 UMI or more than 25% of mitochondrial RNAs were filtered out. After filtering a total of 46238 cells were left for subsequent analysis. In order to identify shared clusters of cells collected from different treatments (before and after challenge) and groups (patient and control), the gene-barcode matrix was integrated according to the integration workflow[93] using SCT-transform to normalize and scale the gene-expression and reciprocal PCA (rPCA) instead of CCA, for dimensionality reduction (with 30 principal components). SCT normalised data was then used for further analysis of generated clusters.

Next, principle components analysis (PCA) and UMAP was performed and 30 PCs were used as input for graph-based clustering (resolution = 0.5). In order to assign the resulting 26 clusters to a cell type, differential gene expression was performed using the Wilcox test (FindAllMarkers function, logfc.threshold = 0.25, only.pos = TRUE, min.diff.pct = 0.2, assay = "SCT"). Top 10 gene-markers of each cluster were displayed with the DotPlot function. The number of cells per cluster in each condition was also calculated and plotted using UMAP projection and 'slit.by' options in Seurat.

Cluster 4, 5,13,15,18,22 and 23 showed a typical MPS-like signature and were subset from the rest. To assign them more precisely to canonical MPS subgroups average gene expression of each cluster was calculated and plotted with the pheatmap package, along with a collection of canonical markers from the literature. To have an unbiased approach we also iterated the FindAllMarkers function on this specific subgroup (FindAllMarkers function, logfc.threshold = 0.25, min.diff.pct = 0.2, assay = "SCT") FindAllMarkers compares each cluster to all the others, so in this case a more specific comparison to MPS only clusters will be performed. Top gene-markers per cluster were generated, and sorted by fold change values in descending order. Dot plots and heat maps (DoMultiBarHeatmap function, https://gitcrcm.marseille.inserm.fr/herault/scHSC_herault/blob/ecf93aa2d914d0b3bd508d066ca887717d78b771/R_src/DoMultipleBarHeatmap.R) were then generated from these lists with the Seurat R package.

Cluster 4 and 5 were shown to contain multiple sub-clusters and were therefore individually subset and re-clustered: data was first re-scaled using the SCTtransform function and dimensionality reduction and clustering (res=0.5) was performed as in the general workflow. Differentially expressed genes between sub-clusters were then identified with the FindAllMarkers function without a min.diff.pct threshold, to include genes that are expressed in multiple sub-clusters but at different levels. ALOX15 positive cells (ALOX15_POS) within the cDC2 cell cluster (T5) were subset from ALOX15 negative cells (ALOX15_NEG) with the WhichCells function and a metadata field based on ALOX15 expression was added. Differentially expressed genes between the two subsets were determined with the FindAllMarkers function.

Each MPS cluster was analyzed to identify differentially expressed genes between conditions in each cell type (cluster). A combined metadata field was added, containing the combination of the cluster, the group (patient/control) and the treatment (before/after challenge) information. In this way the FindMarkers function in Seurat allowed the identification of DEG genes between 2 different subgroups of the same cell type (e.g 'control_Before_4' and 'control_After_4' indicate a comparison between the control group before and after challenge for cluster 4). The test used for analysis between before and after challenge was the LR (linear regression method) that allowed the inclusion of donor information as a latent variable, to correct for an uneven donor distribution in some of the clusters between timepoints. For this analysis we used the RNA assay in the FindMarkers function.

Gene Ontology Enrichment Analysis

Enrichr (amp.pharm.mssm.edu/lib/chea.jsp)[94] gene ontology enrichment analysis was performed on the top 15 (as sorted by absolute log2 fold change) significantly differentially expressed genes (adjusted p-value <0.05) of each major cluster within the MPS compartment (4, 5, 13, 15, 18, 22, 23) to determine the association with specific cell types, based on annotations in the Human Cell Atlas and ARCHS4 tissue databases. The terms with the highest combined score (calculated by multiplying the log of the p-value of the Fishers exact test by the z-score of the deviation from the expected rank) were selected for visualization.

In order to phenotype/identify the individual cell clusters generated by sub-clustering the cDC2 (cluster 5) and $CD14^+$ monocyte (cluster 4) populations, Gene Ontology (GO) enrichment analysis of biological processes (BP) protein complex database (CORUM) and Reactome pathways was performed with g:profiler[95] on the top 40 (as sorted by absolute log2 fold change) significantly differentially expressed genes (adjusted p-value <0.05) between sub-clusters. Genes were analyzed as an unordered query using g:profiler's default g:SCS threshold based methods to correct for multiple testing, and all annotated genes detected in the transcriptomic data as a background set. Lists of enriched Gene Ontology categories were collapsed and simplified with Revigo (http://revigo.irb.hr)[96] using the Homo sapiens set of GO terms. GO terms with dispensability values less than or equal to 0.5 were then visualized in a dot plot (ggplot function, RStudio version 4.0), depicting the negative adjusted Log10 p value and the gene ratio, which equals the number of differentially expressed genes against the number of genes associated with the GO term.

Statistical Analysis

Analysis of all cell frequency data was done with two-tailed, Wilcoxon matched-pairs signed rank test, or Mann-Whitney test with a 95% confidence interval (Prism, GraphPad Software). $p < 0.05$ was considered significant: *$p < 0.05$; **$p < 0.01$;***$p<0.001$. Median and interquartile are range shown in the bar graphs.

References

1. van Furth R, Cohn ZA, Hirsch JG, Humphrey JH, Spector WG, Langevoort HL. The mononuclear phagocyte system: a new classification of macrophages, monocytes, and their precursor cells. *Bull World Health Organ* 1972; **46**(6): 845-52.
2. Desch AN, Gibbings SL, Goyal R, et al. Flow Cytometric Analysis of Mononuclear Phagocytes in Nondiseased Human Lung and Lung-Draining Lymph Nodes. *Am J Respir Crit Care Med* 2016; **193**(6): 614-26.
3. Murray PJ, Allen JE, Biswas SK, et al. Macrophage activation and polarization: nomenclature and experimental guidelines. *Immunity* 2014; **41**(1): 14-20.
4. Bassler K, Schulte-Schrepping J, Warnat-Herresthal S, Aschenbrenner AC, Schultze JL. The Myeloid Cell Compartment-Cell by Cell. *Annu Rev Immunol* 2019; **37**: 269-93.
5. Jakubzick C, Gautier EL, Gibbings SL, et al. Minimal differentiation of classical monocytes as they survey steady-state tissues and transport antigen to lymph nodes. *Immunity* 2013; **39**(3): 599-610.
6. Yona S, Kim KW, Wolf Y, et al. Fate mapping reveals origins and dynamics of monocytes and tissue macrophages under homeostasis. *Immunity* 2013; **38**(1): 79-91.
7. Guilliams M, Mildner A, Yona S. Developmental and Functional Heterogeneity of Monocytes. *Immunity* 2018; **49**(4): 595-613.
8. Kaiko GE, Horvat JC, Beagley KW, Hansbro PM. Immunological decision-making: how does the immune system decide to mount a helper T-cell response? *Immunology* 2008; **123**(3): 326-38.
9. Domogalla MP, Rostan PV, Raker VK, Steinbrink K. Tolerance through Education: How Tolerogenic Dendritic Cells Shape Immunity. *Front Immunol* 2017; **8**: 1764.
10. Thaiss CA, Zmora N, Levy M, Elinav E. The microbiome and innate immunity. *Nature* 2016; **535**(7610): 65-74.
11. de Waal Malefyt R, Abrams J, Bennett B, Figdor CG, de Vries JE. Interleukin 10(IL-10) inhibits cytokine synthesis by human monocytes: an autoregulatory role of IL-10 produced by monocytes. *J Exp Med* 1991; **174**(5): 1209-20.
12. Said EA, Dupuy FP, Trautmann L, et al. Programmed death-1-induced interleukin-10 production by monocytes impairs CD4+ T cell activation during HIV infection. *Nat Med* 2010; **16**(4): 452-9.
13. Xu W, Roos A, Schlagwein N, Woltman AM, Daha MR, van Kooten C. IL-10-producing macrophages preferentially clear early apoptotic cells. *Blood* 2006; **107**(12): 4930-7.
14. Schiller HB, Montoro DT, Simon LM, et al. The Human Lung Cell Atlas: A High-Resolution Reference Map of the Human Lung in Health and Disease. *Am J Respir Cell Mol Biol* 2019; **61**(1): 31-41.
15. Vieira Braga FA, Kar G, Berg M, et al. A cellular census of human lungs identifies novel cell states in health and in asthma. *Nat Med* 2019; **25**(7): 1153-63.
16. Lebel B, Bousquet J, Morel A, Chanal I, Godard P, Michel FB. Correlation between symptoms and the threshold for release of mediators in nasal secretions during nasal challenge with grass-pollen grains. *J Allergy Clin Immunol* 1988; **82**(5 Pt 1): 869-77.
17. Wambre E, Bajzik V, DeLong JH, et al. A phenotypically and functionally distinct human TH2 cell subpopulation is associated with allergic disorders. *Sci Transl Med* 2017; **9**(401).
18. Villani AC, Satija R, Reynolds G, et al. Single-cell RNA-seq reveals new types of human blood dendritic cells, monocytes, and progenitors. *Science* 2017; **356**(6335).
19. Collin M, Bigley V. Human dendritic cell subsets: an update. *Immunology* 2018; **154**(1): 3-20.
20. Mitsi E, Kamng'ona R, Rylance J, et al. Human alveolar macrophages predominately express combined classical M1 and M2 surface markers in steady state. *Respir Res* 2018; **19**(1): 66.
21. Reyfman PA, Walter JM, Joshi N, et al. Single-Cell Transcriptomic Analysis of Human Lung Provides Insights into the Pathobiology of Pulmonary Fibrosis. *Am J Respir Crit Care Med* 2019; **199**(12): 1517-36.
22. Beyer M, Mallmann MR, Xue J, et al. High-resolution transcriptome of human macrophages. *PLoS One* 2012; **7**(9): e45466.
23. See P, Dutertre CA, Chen J, et al. Mapping the human DC lineage through the integration of high-dimensional techniques. *Science* 2017; **356**(6342).

24. Yang J, Anholts J, Kolbe U, Stegehuis-Kamp JA, Claas FHJ, Eikmans M. Calcium-Binding Proteins S100A8 and S100A9: Investigation of Their Immune Regulatory Effect in Myeloid Cells. *Int J Mol Sci* 2018; **19**(7).
25. Zhao F, Hoechst B, Duffy A, et al. S100A9 a new marker for monocytic human myeloid-derived suppressor cells. *Immunology* 2012; **136**(2): 176-83.
26. Mengos AE, Gastineau DA, Gustafson MP. The CD14(+)HLA-DR(lo/neg) Monocyte: An Immunosuppressive Phenotype That Restrains Responses to Cancer Immunotherapy. *Front Immunol* 2019; **10**: 1147.
27. Dorhoi A, Du Plessis N. Monocytic Myeloid-Derived Suppressor Cells in Chronic Infections. *Front Immunol* 2017; **8**: 1895.
28. Kolahian S, Oz HH, Zhou B, Griessinger CM, Rieber N, Hartl D. The emerging role of myeloid-derived suppressor cells in lung diseases. *Eur Respir J* 2016; **47**(3): 967-77.
29. Apodaca MC, Wright AE, Riggins AM, et al. Characterization of a whole blood assay for quantifying myeloid-derived suppressor cells. *J Immunother Cancer* 2019; **7**(1): 230.
30. Kadrmas JL, Beckerle MC. The LIM domain: from the cytoskeleton to the nucleus. *Nat Rev Mol Cell Biol* 2004; **5**(11): 920-31.
31. Cousins RJ, Lanningham-Foster L. Regulation of cysteine-rich intestinal protein, a zinc finger protein, by mediators of the immune response. *J Infect Dis* 2000; **182 Suppl 1**: S81-4.
32. Lanningham-Foster L, Green CL, Langkamp-Henken B, et al. Overexpression of CRIP in transgenic mice alters cytokine patterns and the immune response. *Am J Physiol Endocrinol Metab* 2002; **282**(6): E1197-203.
33. Brown CC, Gudjonson H, Pritykin Y, et al. Transcriptional Basis of Mouse and Human Dendritic Cell Heterogeneity. *Cell* 2019; **179**(4): 846-63 e24.
34. Dutertre CA, Becht E, Irac SE, et al. Single-Cell Analysis of Human Mononuclear Phagocytes Reveals Subset-Defining Markers and Identifies Circulating Inflammatory Dendritic Cells. *Immunity* 2019; **51**(3): 573-89 e8.
35. Bourdely P, Anselmi G, Vaivode K, et al. Transcriptional and Functional Analysis of CD1c(+) Human Dendritic Cells Identifies a CD163(+) Subset Priming CD8(+)CD103(+) T Cells. *Immunity* 2020; **53**(2): 335-52 e8.
36. van Montfoort N, t Hoen PA, Mangsbo SM, et al. Fcgamma receptor IIb strongly regulates Fcgamma receptor-facilitated T cell activation by dendritic cells. *J Immunol* 2012; **189**(1): 92-101.
37. George T, Bell M, Chakraborty M, Siderovski DP, Giembycz MA, Newton R. Protective Roles for RGS2 in a Mouse Model of House Dust Mite-Induced Airway Inflammation. *PLoS One* 2017; **12**(1): e0170269.
38. Gueguen C, Bouley J, Moussu H, et al. Changes in markers associated with dendritic cells driving the differentiation of either TH2 cells or regulatory T cells correlate with clinical benefit during allergen immunotherapy. *J Allergy Clin Immunol* 2016; **137**(2): 545-58.
39. Platzer B, Baker K, Vera MP, et al. Dendritic cell-bound IgE functions to restrain allergic inflammation at mucosal sites. *Mucosal Immunol* 2015; **8**(3): 516-32.
40. Munawara U, Perveen K, Small AG, et al. Human Dendritic Cells Express the Complement Receptor Immunoglobulin Which Regulates T Cell Responses. *Front Immunol* 2019; **10**: 2892.
41. Xu S, Sun Z, Li L, et al. Induction of T cells suppression by dendritic cells transfected with VSIG4 recombinant adenovirus. *Immunol Lett* 2010; **128**(1): 46-50.
42. Zimmer A, Bouley J, Le Mignon M, et al. A regulatory dendritic cell signature correlates with the clinical efficacy of allergen-specific sublingual immunotherapy. *J Allergy Clin Immunol* 2012; **129**(4): 1020-30.
43. Masten BJ, Olson GK, Tarleton CA, et al. Characterization of myeloid and plasmacytoid dendritic cells in human lung. *J Immunol* 2006; **177**(11): 7784-93.
44. van Haarst JM, Verhoeven GT, de Wit HJ, Hoogsteden HC, Debets R, Drexhage HA. CD1a+ and CD1a- accessory cells from human bronchoalveolar lavage differ in allostimulatory potential and cytokine production. *Am J Respir Cell Mol Biol* 1996; **15**(6): 752-9.
45. Wacleche VS, Cattin A, Goulet JP, et al. CD16(+) monocytes give rise to CD103(+)RALDH2(+)TCF4(+) dendritic cells with unique transcriptional and immunological features. *Blood Adv* 2018; **2**(21): 2862-78.
46. Tel-Karthaus N, Kers-Rebel ED, Looman MW, Ichinose H, de Vries CJ, Ansems M. Nuclear Receptor Nur77 Deficiency Alters Dendritic Cell Function. *Front Immunol* 2018; **9**: 1797.

47. Torres-Aguilar H, Aguilar-Ruiz SR, Gonzalez-Perez G, et al. Tolerogenic dendritic cells generated with different immunosuppressive cytokines induce antigen-specific anergy and regulatory properties in memory CD4+ T cells. *J Immunol* 2010; **184**(4): 1765-75.
48. Yue Y, Huang W, Liang J, et al. IL4I1 Is a Novel Regulator of M2 Macrophage Polarization That Can Inhibit T Cell Activation via L-Tryptophan and Arginine Depletion and IL-10 Production. *PLoS One* 2015; **10**(11): e0142979.
49. Romagnani S. IL4I1: Key immunoregulator at a crossroads of divergent T-cell functions. *Eur J Immunol* 2016; **46**(10): 2302-5.
50. Zhang S, Yu M, Guo Q, et al. Annexin A2 binds to endosomes and negatively regulates TLR4-triggered inflammatory responses via the TRAM-TRIF pathway. *Sci Rep* 2015; **5**: 15859.
51. Sands MF, Ohtake PJ, Mahajan SD, et al. Tissue inhibitor of metalloproteinase-1 modulates allergic lung inflammation in murine asthma. *Clin Immunol* 2009; **130**(2): 186-98.
52. Francesca Fallarino MG, Carlos Briseno, Peter Murray, Giulia Scalisi, Antonella Turco, Davide Matino, Paolo Puccetti, Theresa L Murphy and Kenneth M Murphy. Deciphering Interleukin 4-induced gene-1 as novel immune regulatory pathway in dendritic cell subsets. *Journal of Immunology* 2017; **198**(1).
53. Fan C, Zhang X, Zhang P, et al. LPS stimulation during HCV infection induces MMP/TIMP1 imbalance in macrophages. *J Med Microbiol* 2020; **69**(5): 759-66.
54. Zhu N, Zhang GX, Yi B, et al. Nur77 limits endothelial barrier disruption to LPS in the mouse lung. *Am J Physiol Lung Cell Mol Physiol* 2019; **317**(5): L615-L24.
55. Pei L, Castrillo A, Chen M, Hoffmann A, Tontonoz P. Induction of NR4A orphan nuclear receptor expression in macrophages in response to inflammatory stimuli. *J Biol Chem* 2005; **280**(32): 29256-62.
56. Granot T, Senda T, Carpenter DJ, et al. Dendritic Cells Display Subset and Tissue-Specific Maturation Dynamics over Human Life. *Immunity* 2017; **46**(3): 504-15.
57. Tanne B, Bernier S, Dumais N. CCR7 Receptor Expression in Mono-MAC-1 Cells: Modulation by Liver X Receptor alpha Activation and Prostaglandin E 2. *Int J Inflam* 2015; **2015**: 201571.
58. Jardine L, Wiscombe S, Reynolds G, et al. Lipopolysaccharide inhalation recruits monocytes and dendritic cell subsets to the alveolar airspace. *Nat Commun* 2019; **10**(1): 1999.
59. Ben J, Jiang B, Wang D, et al. Major vault protein suppresses obesity and atherosclerosis through inhibiting IKK-NF-kappaB signaling mediated inflammation. *Nat Commun* 2019; **10**(1): 1801.
60. Wang J, Cui Z, Liu L, et al. MiR-146a mimic attenuates murine allergic rhinitis by downregulating TLR4/TRAF6/NF-kappaB pathway. *Immunotherapy* 2019; **11**(13): 1095-105.
61. Gubernatorova EO, Gorshkova EA, Namakanova OA, et al. Non-redundant Functions of IL-6 Produced by Macrophages and Dendritic Cells in Allergic Airway Inflammation. *Front Immunol* 2018; **9**: 2718.
62. Schulthess J, Pandey S, Capitani M, et al. The Short Chain Fatty Acid Butyrate Imprints an Antimicrobial Program in Macrophages. *Immunity* 2019; **50**(2): 432-45 e7.
63. Trompette A, Gollwitzer ES, Pattaroni C, et al. Dietary Fiber Confers Protection against Flu by Shaping Ly6c(-) Patrolling Monocyte Hematopoiesis and CD8(+) T Cell Metabolism. *Immunity* 2018; **48**(5): 992-1005 e8.
64. Trompette A, Gollwitzer ES, Yadava K, et al. Gut microbiota metabolism of dietary fiber influences allergic airway disease and hematopoiesis. *Nat Med* 2014; **20**(2): 159-66.
65. Durack J, Lynch SV, Nariya S, et al. Features of the bronchial bacterial microbiome associated with atopy, asthma, and responsiveness to inhaled corticosteroid treatment. *J Allergy Clin Immunol* 2017; **140**(1): 63-75.
66. Budden KF, Shukla SD, Rehman SF, et al. Functional effects of the microbiota in chronic respiratory disease. *Lancet Respir Med* 2019; **7**(10): 907-20.
67. Kapellos TS, Bonaguro L, Gemund I, et al. Human Monocyte Subsets and Phenotypes in Major Chronic Inflammatory Diseases. *Front Immunol* 2019; **10**: 2035.
68. Linton L, Karlsson M, Grundstrom J, et al. HLA-DR(hi) and CCR9 Define a Pro-Inflammatory Monocyte Subset in IBD. *Clin Transl Gastroenterol* 2012; **3**: e29.
69. Randolph GJ, Sanchez-Schmitz G, Liebman RM, Schakel K. The CD16(+) (FcgammaRIII(+)) subset of human monocytes preferentially becomes migratory dendritic cells in a model tissue setting. *J Exp Med* 2002; **196**(4): 517-27.

70. Sanchez-Torres C, Garcia-Romo GS, Cornejo-Cortes MA, Rivas-Carvalho A, Sanchez-Schmitz G. CD16+ and CD16- human blood monocyte subsets differentiate in vitro to dendritic cells with different abilities to stimulate CD4+ T cells. *Int Immunol* 2001; **13**(12): 1571-81.
71. Rivas-Carvalho A, Meraz-Rios MA, Santos-Argumedo L, et al. CD16+ human monocyte-derived dendritic cells matured with different and unrelated stimuli promote similar allogeneic Th2 responses: regulation by pro- and anti-inflammatory cytokines. *Int Immunol* 2004; **16**(9): 1251-63.
72. Reinartz SM, van Tongeren J, van Egmond D, de Groot EJ, Fokkens WJ, van Drunen CM. Dendritic cells in nasal mucosa of subjects with different allergic sensitizations. *J Allergy Clin Immunol* 2011; **128**(4): 887-90.
73. KleinJan A, Willart M, van Rijt LS, et al. An essential role for dendritic cells in human and experimental allergic rhinitis. *J Allergy Clin Immunol* 2006; **118**(5): 1117-25.
74. Bachus H, Kaur K, Papillion AM, et al. Impaired Tumor-Necrosis-Factor-alpha-driven Dendritic Cell Activation Limits Lipopolysaccharide-Induced Protection from Allergic Inflammation in Infants. *Immunity* 2019; **50**(1): 225-40 e4.
75. van den Brink SC, Sage F, Vertesy A, et al. Single-cell sequencing reveals dissociation-induced gene expression in tissue subpopulations. *Nat Methods* 2017; **14**(10): 935-6.
76. Eguiluz-Gracia I, Bosco A, Dollner R, et al. Rapid recruitment of CD14(+) monocytes in experimentally induced allergic rhinitis in human subjects. *J Allergy Clin Immunol* 2016; **137**(6): 1872-81 e12.
77. Melum GR, Farkas L, Scheel C, et al. A thymic stromal lymphopoietin-responsive dendritic cell subset mediates allergic responses in the upper airway mucosa. *J Allergy Clin Immunol* 2014; **134**(3): 613-21 e7.
78. Jahnsen FL, Lund-Johansen F, Dunne JF, Farkas L, Haye R, Brandtzaeg P. Experimentally induced recruitment of plasmacytoid (CD123high) dendritic cells in human nasal allergy. *J Immunol* 2000; **165**(7): 4062-8.
79. Coillard A, Segura E. In vivo Differentiation of Human Monocytes. *Front Immunol* 2019; **10**: 1907.
80. Kim OY, Monsel A, Bertrand M, Coriat P, Cavaillon JM, Adib-Conquy M. Differential down-regulation of HLA-DR on monocyte subpopulations during systemic inflammation. *Crit Care* 2010; **14**(2): R61.
81. Meisel C, Schefold JC, Pschowski R, et al. Granulocyte-macrophage colony-stimulating factor to reverse sepsis-associated immunosuppression: a double-blind, randomized, placebo-controlled multicenter trial. *Am J Respir Crit Care Med* 2009; **180**(7): 640-8.
82. Gomez HG, Gonzalez SM, Londono JM, et al. Immunological characterization of compensatory anti-inflammatory response syndrome in patients with severe sepsis: a longitudinal study*. *Crit Care Med* 2014; **42**(4): 771-80.
83. Stein MM, Hrusch CL, Gozdz J, et al. Innate Immunity and Asthma Risk in Amish and Hutterite Farm Children. *N Engl J Med* 2016; **375**(5): 411-21.
84. Schuijs MJ, Willart MA, Vergote K, et al. Farm dust and endotoxin protect against allergy through A20 induction in lung epithelial cells. *Science* 2015; **349**(6252): 1106-10.
85. Qian G, Jiang W, Zou B, et al. LPS inactivation by a host lipase allows lung epithelial cell sensitization for allergic asthma. *J Exp Med* 2018; **215**(9): 2397-412.
86. Imran S, Neeland MR, Shepherd R, et al. A Potential Role for Epigenetically Mediated Trained Immunity in Food Allergy. *iScience* 2020; **23**(6): 101171.
87. Bousquet J, Khaltaev N, Cruz AA, et al. Allergic Rhinitis and its Impact on Asthma (ARIA) 2008 update (in collaboration with the World Health Organization, GA(2)LEN and AllerGen). *Allergy* 2008; **63 Suppl 86**: 8-160.
88. Terreehorst I, Oosting AJ, Tempels-Pavlica Z, et al. Prevalence and severity of allergic rhinitis in house dust mite-allergic patients with bronchial asthma or atopic dermatitis. *Clin Exp Allergy* 2002; **32**(8): 1160-5.
89. Boot JD, Chandoesing P, de Kam ML, et al. Applicability and reproducibility of biomarkers for the evaluation of anti-inflammatory therapy in allergic rhinitis. *J Investig Allergol Clin Immunol* 2008; **18**(6): 433-42.
90. de Graaf-in't Veld C, Garrelds IM, van Toorenenbergen AW, Gerth van Wijk R. Nasal responsiveness to allergen and histamine in patients with perennial rhinitis with and without a late phase response. *Thorax* 1997; **52**(2): 143-8.
91. Bagwell B. A New Analytic Approach for Live Singlet Identification. 2017. https://www.fluidigm.com/ articles/mass-cyto-summit-videos?mkt__tok=eyJpIjoiT0RVeU5ERTBNbU5o

WW1GbSIsInQiOiJ4U3NDdUZjbVoyRCt6UThrWXg4b3M3RUNick5ZK0l
sekJZQzU3VFZyU0QwYW5UaHdaQUxwbDh3ZHJzbTRcLzg3MlhlWkh5b
EFDMUdWSFk0NWpiTmhueGVXQ3IzQzI4K0Q5a015cGM1bFdrVHl2elp
NY2JGUERqb2I3MEk0RW9FemgifQ%3D%3D#bagwell (accessed June, 2018.
92. Beyrend G, Stam K, Hollt T, Ossendorp F, Arens R. Cytofast: A workflow for visual and quantitative analysis of flow and mass cytometry data to discover immune signatures and correlations. *Comput Struct Biotechnol J* 2018; **16**: 435-42.
93. Stuart T, Butler A, Hoffman P, et al. Comprehensive Integration of Single-Cell Data. *Cell* 2019; **177**(7): 1888-902 e21.
94. Kuleshov MV, Jones MR, Rouillard AD, et al. Enrichr: a comprehensive gene set enrichment analysis web server 2016 update. *Nucleic Acids Res* 2016; **44**(W1): W90-7.
95. Raudvere U, Kolberg L, Kuzmin I, et al. g:Profiler: a web server for functional enrichment analysis and conversions of gene lists (2019 update). *Nucleic Acids Res* 2019; **47**(W1): W191-W8.
96. Supek F, Bosnjak M, Skunca N, Smuc T. REVIGO summarizes and visualizes long lists of gene ontology terms. *PLoS One* 2011; **6**(7): e21800.

Figure 1

A

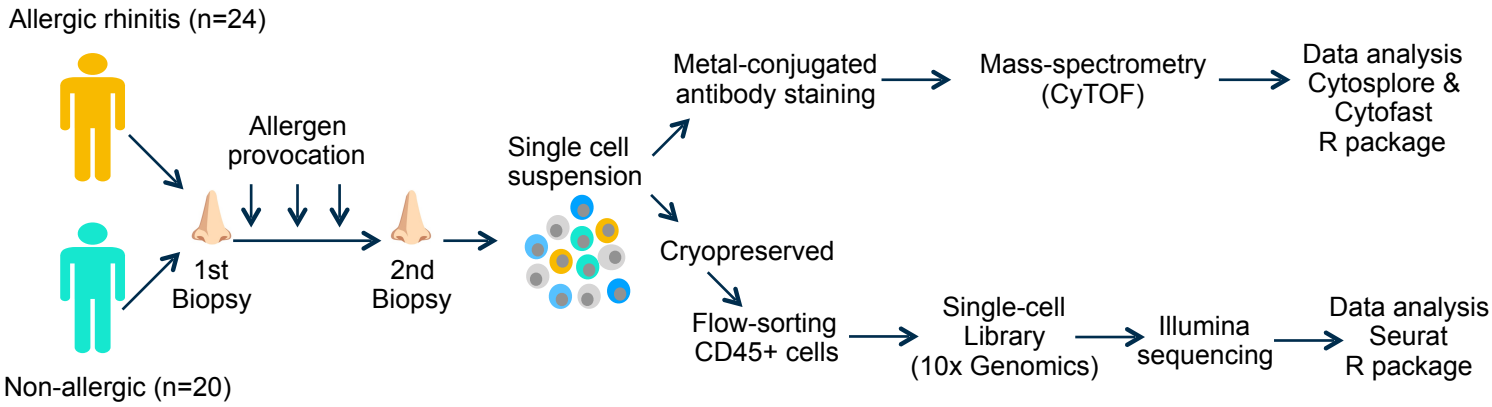

B

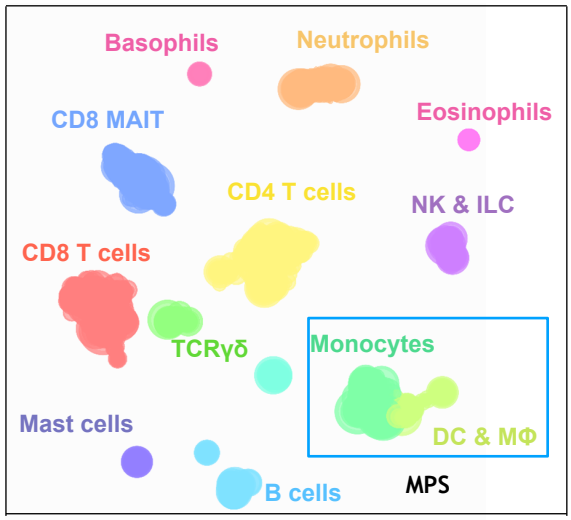

29 donors; 53 samples; 752,348 cells

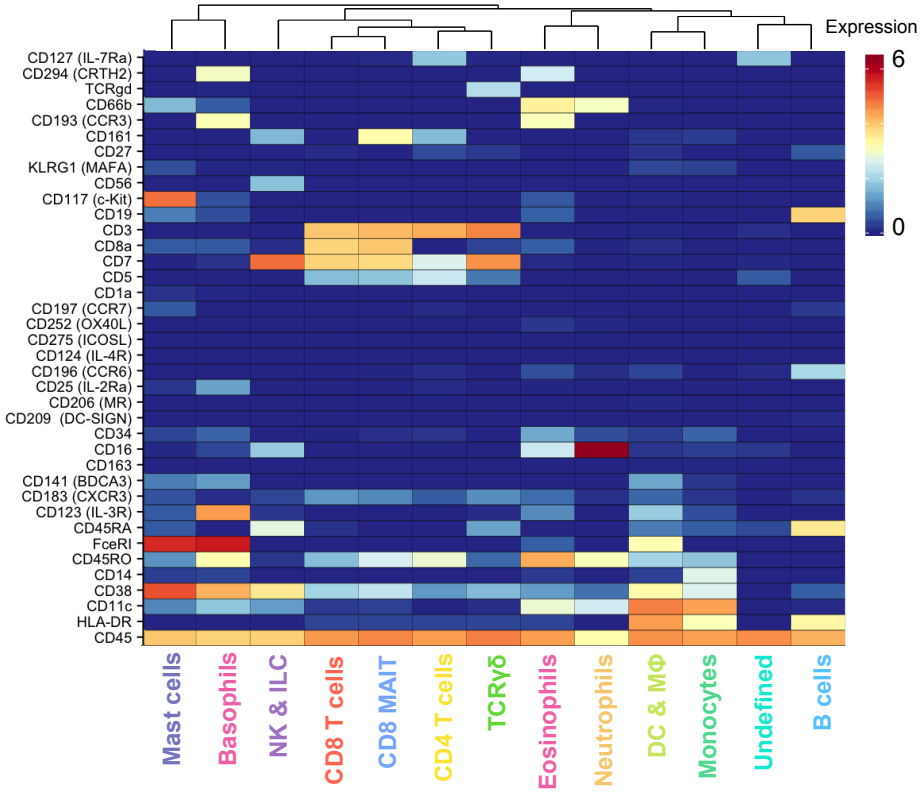

C

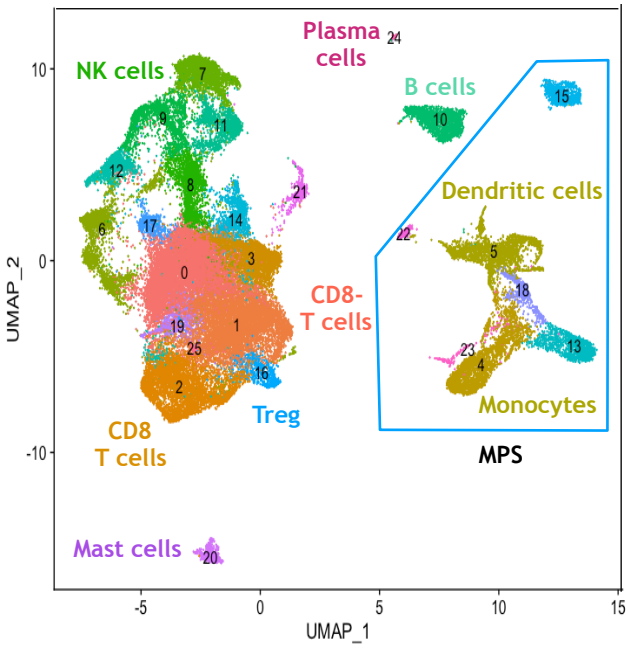

39 donors; 75 samples; 46,238 cells

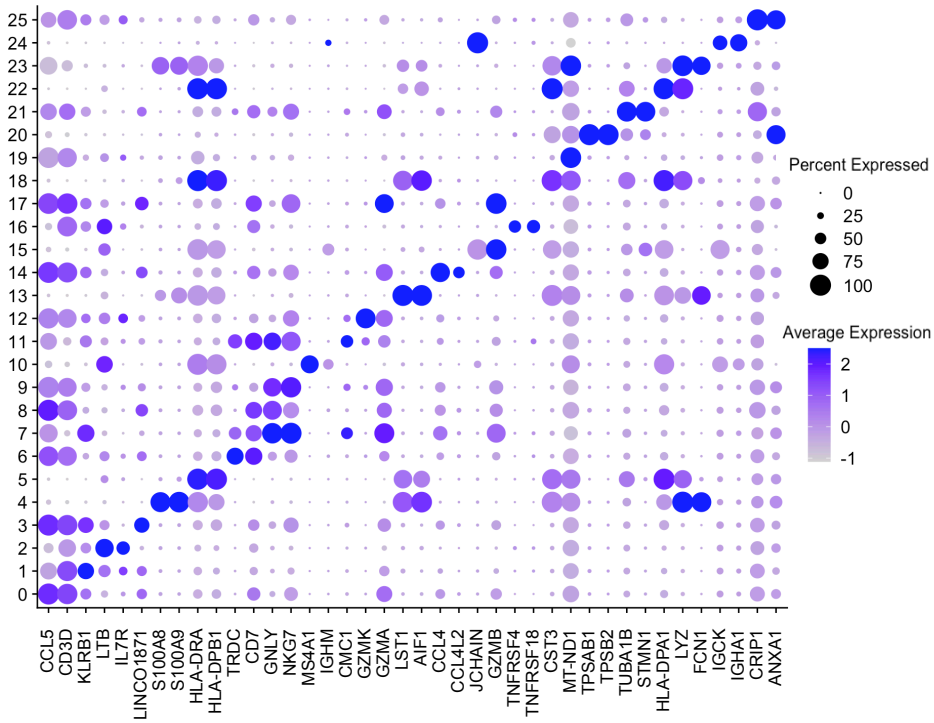

Figure 2

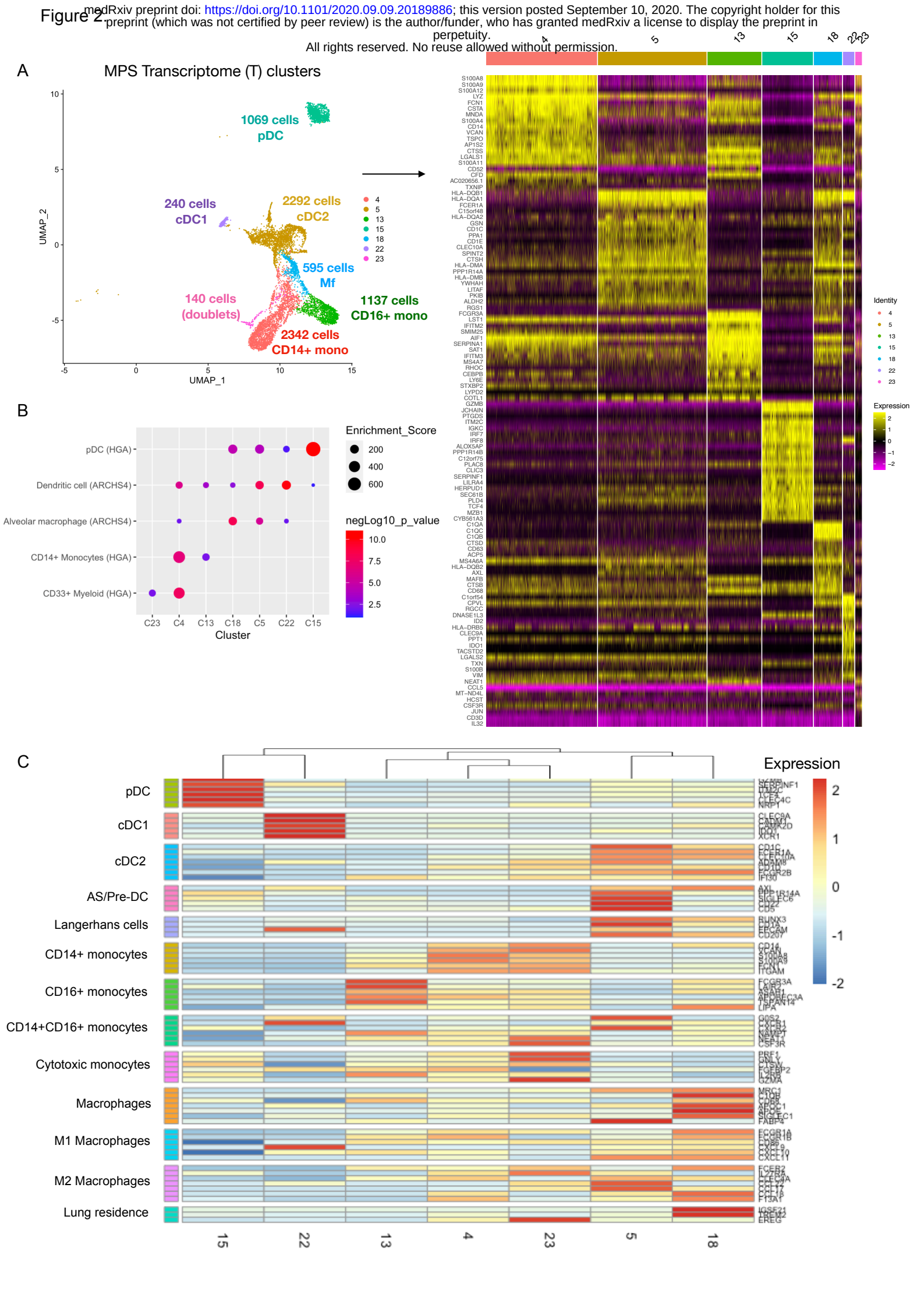

Figure 3:

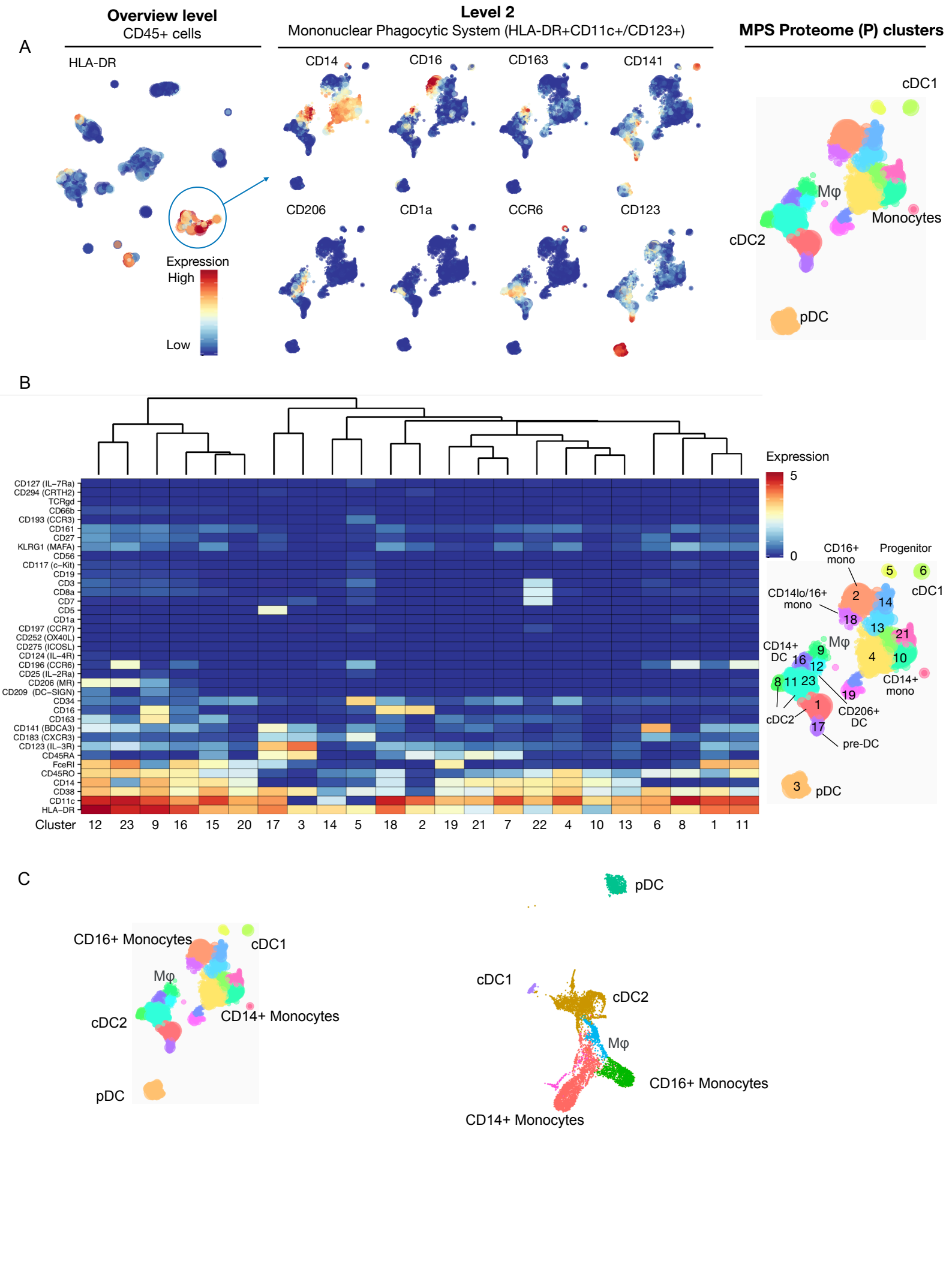

Figure 4.

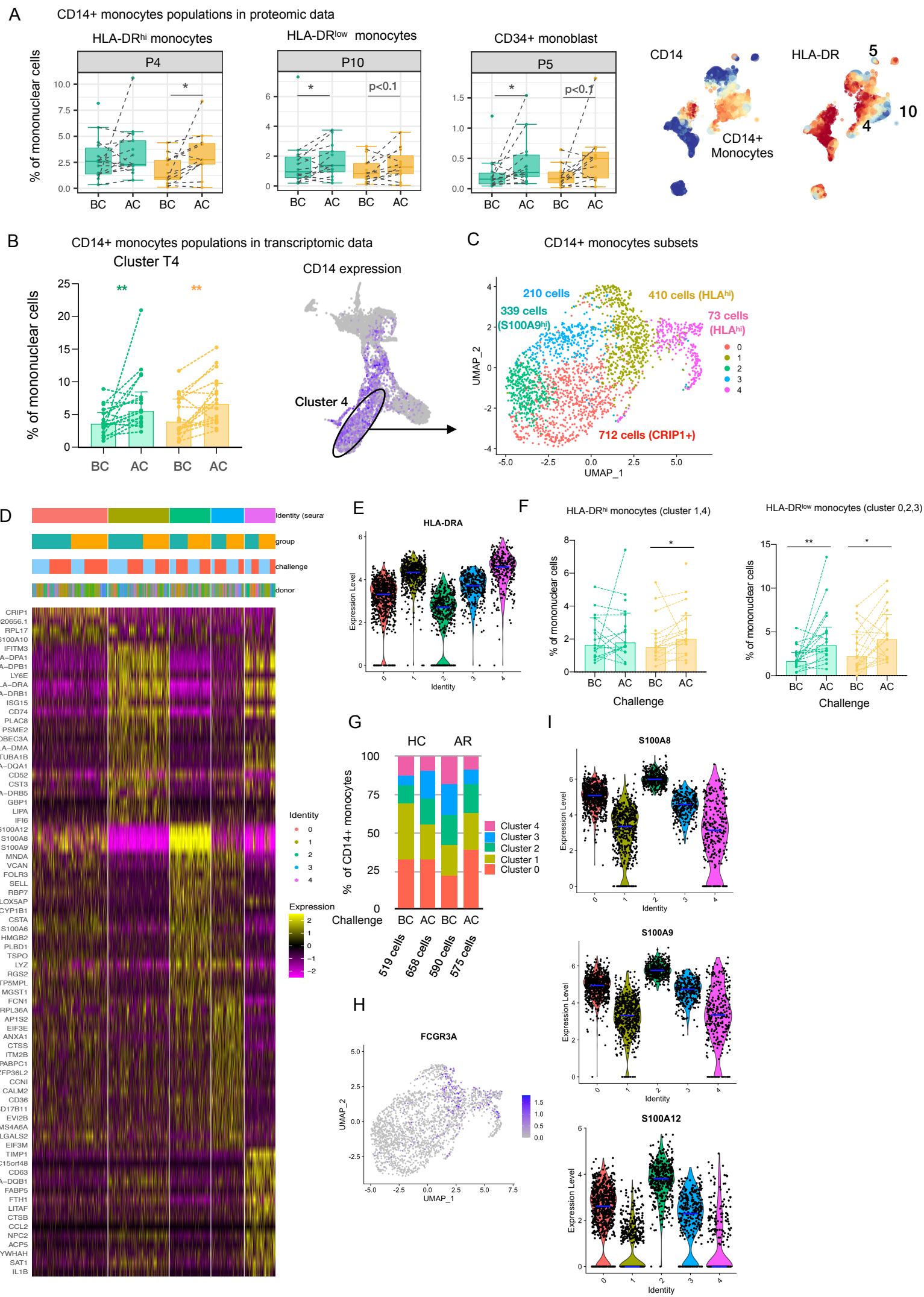

Figure 5.

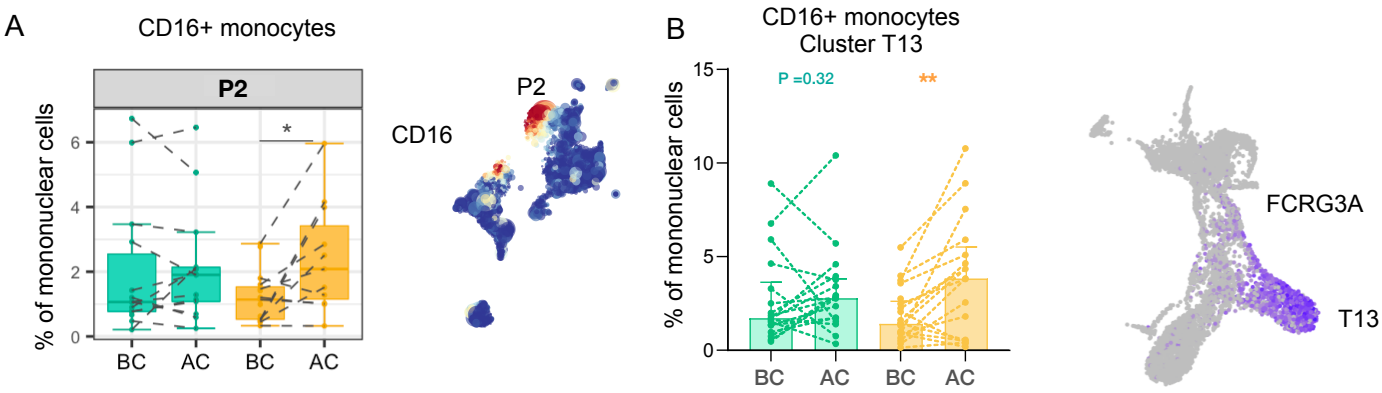

Figure 6

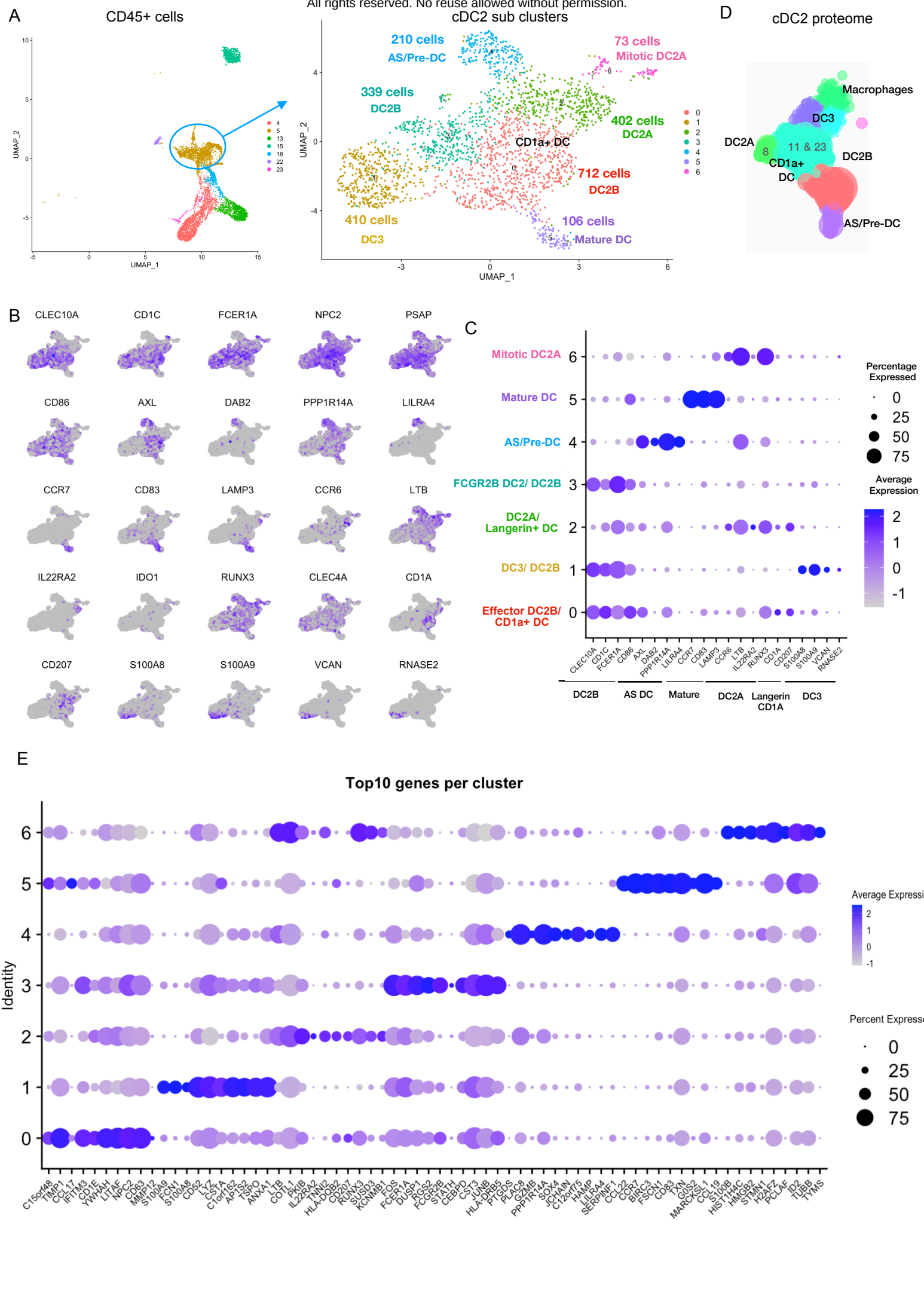

Figure 6: (continued)

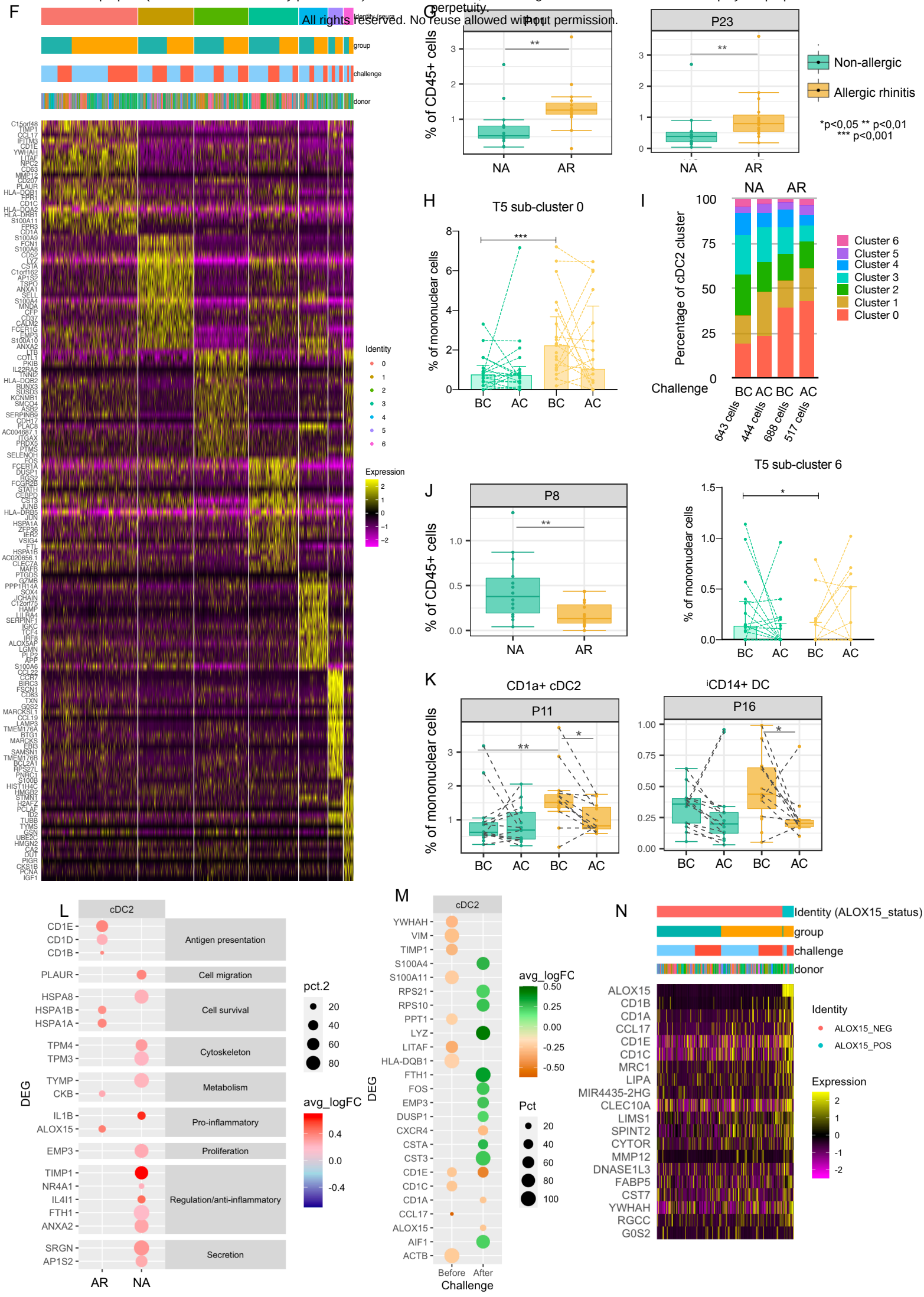

Table 1

	Non-allergic	Allergic rhinitis
CyTOF Cohort		
Number of subjects	14 (1 WD)	15 (4 WD)
Female (%)	64,3	46,7
Median age (min-max)	23 (18-49)	26 (18-45)
Median SPT (HDM)	Negative (<0.4)	1,01 (0,47-3,47)
Median HDM-specific serum IgE (CAPFEIA)	Negative (< 0,35 KU/l)	12,7 (0,39- >100)
Median symptom score	Negative (<5)	18 (11-28)
scRNAseq Cohort		
Number of subjects	18	21
Female (%)	61,1	52,4
Median age (min-max)	25 (19-49)	24 (18-45)
Median SPT (HDM)	Negative (<0.4)	1,01 (0,46-2,48)
Median HDM-specific serum IgE (CAPFEIA)	Negative (< 0,35 KU/l)	8,9 (0,39- >100)
Median symptom score	Negative (<5)	18 (9-28)
Cohort overlap	12	12

Figure Legends

Figure 1. Study set up, cell clustering and lineage identification

A. Schematic of study design and protocol for single cell transcriptomic and proteomic data collection and analysis of nasal biopsy cells from allergic and non-allergic individuals.
B. HSNE plot of cell lineages identified in proteomic data and heatmap of markers used. MPS cells, based on HLA-DR and CD11c or CD123, are indicated in the blue box within the HSNE plot.
C. UMAP of cell lineages identified in proteomic data and dot plot representing the top two markers of each cluster sorted by log fold change. MPS cells, expressing LYZ and/or CST3 together with HLA-DR/CD74 are indicated in the blue box within the HSNE plot.

Figure 2. MPS cell cluster annotation in transcriptomic data.

A. UMAP of MPS clusters with accompanying heat map of top 10 marker genes sorted by log fold change of each of the clusters within the MPS compartment.
B. Dot plot of Gene Ontology Enrichment analysis performed in Enrichr on the top 40 markers obtained for each MPS cell cluster, showing the top combined score for each cluster. Human cell atlas and ARCHS4 Tissue gene set libraries were used for enrichment analysis.
C. Heat map of average expression for each MPS cluster (identity listed below) of signature genes (listed on the right) of known cell types (listed on the left).

Figure 3. MPS cell cluster annotation in proteomic data.

A. MPS cell location in HSNE plot and expression of relevant markers for major MPS cell type identification.
B. Heat map of cell marker expression in proteomic data with identification of DC, monocyte and macrophage populations.
C. Alignment of major MPS cell populations between proteomic and transcriptomic data sets.

Figure 4. Recruitment of different monocyte populations in response to allergen challenge.

A. Box plots of frequency of HLA-DR^{low} (cluster P5 and P10) and HLA-DR^{hi} CD14+ monocytes (cluster P4) in allergic (orange boxes) and non-allergic individuals (green boxes) before (BC) and after allergen challenge (AC) in the proteomic data. * $p < 0.05$
B. Box plots of frequency of CD14+ monocytes (Cluster T4) in allergic (orange boxes) and non-allergic individuals (green boxes) before (BC) and after allergen challenge (AC) in the transcriptomic data. ** $p < 0.01$
C. UMAP of five sub-clusters generated from CD14+ monocytes, cluster T4 of the original clusters. Total cell number and distinguishing marker per sub-cluster depicted in the plot.
D. Heat map of top 20 gene markers sorted by log fold change of the sub-clusters within the CD14+ monocytes. Bars above heat map indicate composition of clusters based on group (allergic in orange; non-allergic in green), allergen challenge (blue before challenge; red after challenge) and donor. Colours of sub-clusters (identity) correspond with those depicted in UMAP in Figure 4C.
E. Violin plot of HLA-DR expression by sub-cluster of CD14+ monocytes.
F. Box plots of frequency of HLA-DR^{low} (sub-cluster 0, 2, 3) and HLA-DR^{hi} CD14+ monocytes (sub-cluster 1, 4) in allergic (orange boxes) and non-allergic individuals (green boxes) before (BC) and after allergen challenge (AC) in the transcriptomic data. * $p < 0.05$, ** $p < 0.01$
G. Composition of CD14+ monocytes by sub-cluster for non-allergic individuals (NA) and allergic individuals (AR), before (BC) and after allergen challenge (AC). Colours of sub-clusters correspond with those depicted in UMAP in Figure 4C.
H. UMAP of FCGR3A expression in sub-clusters of CD14+ monocytes.
I. Violin plot of S100A8, S100A9 and S100A12 expression by sub-cluster of CD14+ monocytes.

Figure 5. Recruitment of CD16+ monocyte populations in allergic individuals

A. Box plot of frequency of CD16+ monocytes (cluster P2) in allergic (orange boxes) and non-allergic individuals (green boxes) before (BC) and after allergen challenge (AC) in the proteomic data. * $p < 0.05$. Expression of CD16 depicted in HSNE, with cluster P2 indicated in the plot.
B. Boxplot of frequency of CD16+ monocytes (cluster T13) in allergic (orange boxes) and non-allergic individuals (green boxes) before (BC) and after allergen challenge (AC) in the transcriptomic data. * *$p < 0.01$. Gene expression of FCGR3A depicted in UMAP, with cluster T13 indicated in the plot.

Figure 6. Differences in the balance between effector and anti-inflammatory cDC2 in allergic and non-allergic subjects

A. UMAP of seven sub-clusters generated from cDC2, cluster T5 of the original clusters. Total cell number and distinguishing marker per sub-cluster depicted in the plot.
B. UMAP of gene expression of established cell type markers.
C. Dot plot of percentage of cells expressing marker genes of established cell types including DC2A, DC2B, DC3, AS DC, mature DC, Langerin+ DC and CD1a+ DC.
D. Alignment of cDC2 cell clusters with those identified in proteomic data.
E. Dot plot representing the top ten markers of each cluster sorted by log fold change for each cDC2 sub-cluster.
F. Heat map of top 20 gene markers sorted by log fold change of the sub-clusters within the cDC2 compartment. Bars above heat map indicate composition of clusters based on group (allergic in orange; non-allergic in green), allergen challenge (blue before challenge; red after challenge) and donor. Colours of sub-clusters (identity) correspond with those depicted in UMAP in Figure 6A.
G. Box plot of frequency of cDC2 clusters P11 and P23 of the proteomic data for in allergic (orange boxes) and non-allergic individuals (green boxes) before allergen challenge. ** $p < 0.01$
H. Box plot of frequency of effector cDC2 (cluster T5, sub-cluster 0) of the transcriptomic data in allergic (orange boxes) and non-allergic individuals (green boxes) before (BC) and after allergen challenge (AC). ** $p < 0.01$
I. Composition of cDC2 by sub-cluster for non-allergic individuals (NA) and allergic individuals (AR), before (BC) and after allergen challenge (AC). Colours of sub-clusters correspond with those depicted in UMAP in Figure 6A.
J. Box plot of frequency of cDC2 clusters P8 of the proteomic data and box plot of frequency of mitotic cDC2A (cluster T5, sub-cluster 6) of the transcriptomic data in allergic (orange boxes) and non-allergic individuals (green boxes) before (BC) and after allergen challenge (AC). * $p < 0.05$, ** $p < 0.01$
K. Box plots of frequency of cDC2 sub-clusters (P11 and P16) in allergic (orange boxes) and non-allergic individuals (green boxes) before (BC) and after allergen challenge (AC) in the proteomic data. * $p < 0.05$, * $p< 0.0$
L. Dot plot of differentially expressed genes in cDC2 cells (Cluster T5) between before and after allergen challenge for allergic (AR) and non-allergic (NA) individuals. Red represents up-regulation of genes, blue represents down-regulation of genes. Colour intensity represent log fold change (with 0.2 cut off). Size of dot represents the percentage of cells genes are expressed in after allergen challenge.
M. Dot plot of differentially expressed genes in cDC2 cells (Cluster T5) between allergic (AR) and non-allergic (NA) individuals, before (BC) and after allergen challenge (AC). Orange represents gene expression higher in allergic individuals, green represents gene expression higher in non-allergic individuals, colour intensity represent log fold change. Size of dot represents the percentage of cells in which the genes are expressed.
N. Heat map of top 20 gene markers sorted by log fold change of ALOX15 expressing cells (green; top bar) compared to ALOX15 negative cells (red; top bar) within the cDC2 compartment. Bars above heat map further indicate composition of clusters based on group (allergic in orange; non-allergic in green), allergen challenge (blue before challenge; red after challenge) and donor.

Table 1. Cohort characteristics